Space Sci Rev (2009) 145: 285–335
DOI 10.1007/s11214-009-9518-5

Time-Dependent Nuclear Decay Parameters: New Evidence for New Forces?

E. Fischbach · J.B. Buncher · J.T. Gruenwald · J.H. Jenkins · D.E. Krause · J.J. Mattes · J.R. Newport

Received: 14 April 2009 / Accepted: 29 April 2009 / Published online: 28 May 2009

Abstract This paper presents an overview of recent research dealing with the question of whether nuclear decay rates (or half-lives) are time-independent constants of nature, as opposed to being parameters which can be altered by an external perturbation. If the latter is the case, this may imply the existence of some new interaction(s) which would be responsible for any observed time variation. Interest in this question has been renewed recently by evidence for a correlation between nuclear decay rates and Earth–Sun distance, and by the observation of a dip in the decay rate for ^{54}Mn coincident in time with the solar flare of 2006 December 13. We discuss these observations in detail, along with other hints in the literature for time-varying decay parameters, in the framework of a general phenomenology that we develop. One consequence of this phenomenology is that it is possible for different experimental groups to infer discrepant (yet technically correct) results for a half-life depending on where and how their data were taken and analyzed. A considerable amount of attention is devoted to possible mechanisms which might give rise to the reported effects, including fluctuations in the flux of solar neutrinos, and possible variations in the magnitudes of fundamental parameters, such as the fine structure constant and the electron-to-proton mass ratio. We also discuss ongoing and future experiments, along with some implications of our work for cancer treatments, ^{14}C dating, and for the possibility of detecting the relic neutrino background.

Keywords Solar physics: Particle emission · Solar physics: Flare · Nuclear reactions: Fluctuation phenomena

E. Fischbach (✉) · J.B. Buncher · J.T. Gruenwald · J.H. Jenkins · J.J. Mattes · J.R. Newport
Physics Department, Purdue University, West Lafayette, IN 47906, USA
e-mail: ephraim@physics.purdue.edu

D.E. Krause
Physics Department, Wabash College, Crawfordsville, IN 47933, USA

1 Introduction

Few issues frame the history of natural radioactivity as fundamentally as the question of whether the decay rates of nuclides are constants of nature, unaffected by the external environment. Following the discovery of radioactivity by Becquerel (1896), an intense effort was mounted to ascertain whether the decay rates of nuclides could be affected by external influences including temperature, pressure, chemical composition, concentration, and magnetic fields. One example of this effort is an experiment carried out by Rutherford (1913, p. 505) who contained a quantity of radon gas in a high pressure bomb along with the explosive cordite. The authors estimated that when the cordite was detonated the maximum temperature in the bomb reached 2500°C, and the pressure ∼1000 atm, and yet the γ-ray activity from the radon was unchanged. By 1930 Rutherford et al. (1930, p. 161) concluded that "The rate of transformation of an element has been found to be a constant under all conditions." The object of the present paper is to revisit this question in light of recent suggestions that some radioactive decays may in fact be affected by solar activity and/or by other external influences.

In order to define the question at hand more precisely it is useful to distinguish among the following modes of nuclear decay, which will be the focus of our discussion; α, $\beta^{\pm}$, and ϵ (electron capture). It is not surprising to find that electron capture rates depend on the environment of the atom: these rates depend on the overlap of the wavefunction of an orbital electron with the nucleus (Wu and Moszkowski 1966, p. 195ff) which can be affected by the local chemical or physical environment of the decaying atom (Emery 1972; Hahn et al. 1976; Norman et al. 2001; Ohtsuki et al. 2004). Similarly, β-decay rates in stars can be influenced by very strong magnetic fields which alter the wavefunctions of the emitted β-particles, and hence the phase space available for the decays (Matese and O'Connell 1969; Fassio-Canuto 1969). In the present paper we will not deal with either of these cases. In the ensuing discussion we will, however, consider in some detail the electron capture process $^{54}\mathrm{Mn} + e^- \rightarrow {}^{54}\mathrm{Cr} + \nu_e$, but only in connection with data we obtained for this decay during the solar flare of 2006 December 13.

This work is an outgrowth of an effort to apply the GRIP randomness test (Tu and Fischbach 2003; Tu and Fischbach 2005) to nuclear decays. Although it is almost universally assumed that nuclear decays are random, experimental tests of this assumption are relatively scant (Anderson and Spangler 1973; Silverman et al. 1999; Silverman et al. 2000). In the course of designing an appropriate experiment based on the GRIP formalism, we came upon a paper by Alburger et al. (1986) which revealed an unexpected annual variation in the decay rates of ^{32}Si and ^{36}Cl (see Sect. 2 below). This experiment, which was carried out at Brookhaven National Laboratory (BNL) between 1982 and 1986, questioned our understanding of nuclear decays, particularly our belief that these decays are uncorrelated in time with any other influence. Further exploration of the literature revealed yet another data set which exhibited an annual variation in decay rates, this from an experiment studying ^{152}Eu, ^{154}Eu, and ^{226}Ra at the Phyikalische-Technische Bundesanstalt (PTB) in Germany. Other researchers have also reported time-varying count-rates, and Table 1 provides a guide to some of these experiments. As we discuss in Sect. 2, the annual variation of the BNL and PTB data, along with the correlation of these data sets with each other, raised the question of whether these decay rates (and possibly others as well) were in fact being influenced by an external source, or whether they simply represented some poorly understood instrumental effects.

The unexpected correlations observed in the BNL and PTB data have served as the motivation for an ongoing series of experiments at Purdue. In one of these, data taken

Table 1 Summary of experiments suggesting a possible time-dependence of nuclear decay rates. For each entry the observed nuclides and their dominant decay modes are exhibited along with the approximate dates when the corresponding experiments were carried out. The decay modes are indicated by α (alpha-decay), β (beta-decay), and ϵ (electron-capture). Observed periodicities in the decay rates are noted. The interested reader is referred to the references for further details

Source	Mode	Duration	Periodicity (d)	Reference
^{3}H	β^-		0.5 y	(Lobashev et al. 1999)$^{\#}$
^{3}H	β^-	Fall 1980–Spring 1982	365	(Falkenberg 2001)*
^{32}Si	β^-	1982–1986	365	(Alburger et al. 1986)
^{60}Co	β^-	1999.06–2001.12	1, ∼30, 365	(Parkhomov 2005)
^{60}Co	β^-	1998.12–1999.04	1, 27	(Baurov et al. 2007)
^{60}Co	β^-	2000.03–2000.04		(Baurov et al. 2001)
^{137}Cs	β^-	1998.12–1999.04	1, 27	(Baurov et al. 2007)
^{137}Cs	β^-	2000.03–2000.04		(Baurov et al. 2001)
^{226}Ra	α	1981–1996	365	(Siegert et al. 1998)
^{238}Pu	α	1978–1980; 1982–7	365	(Ellis 1990)
Various	α, β, ϵ		1, 27, 365	(Shnoll et al. 1998, 2000)†

*Indicates comments on this paper by Bruhn (2002) and Falkenberg (2002), and the †indicates comments by Derbin et al. (2000) and Kushnirenko and Pogozhev (2000). The #denotes that Lobashev et al. (1999) report a periodic effect ("Troitsk anomaly") in the determination of m_ν^2 from ^{3}H β-decay. A recent paper by Kostenko and Yuriev (2008) discusses a possible connection between some of the time-dependence of half-lives reported in this table and magnetic monopoles.

during the solar flare of 2006 December 13 exhibited a dip in the counting rate of a ^{54}Mn sample which coincided in time with the flare. These data are presented and analyzed in Sect. 3. They serve as part of the motivation for the remainder of this paper, where we explore the phenomenology of a time-dependent λ, which is defined by the decay law $\dot{N}(t) \equiv dN(t)/dt = -\lambda(t)N(t)$. Note that the unperturbed half-life $T_{1/2}$ is given by $T_{1/2} = \ln 2/\lambda$. We will henceforth avoid the awkward oxymoronic construction "time-dependent decay constant" by referring to λ as the "decay parameter".

It must be emphasized that even if the correlations reported in the BNL and PTB data prove to be reproducible, and similarly for the solar flare data, this does not necessarily imply that they arise from a time-dependent modification of λ, as described by the phenomenology in Sect. 4 below. The observed effects could arise from a field or particles emanating from the Sun which modify the experimental apparatus rather than λ, or from some conventional, but overlooked, influence on the apparatus arising from local fluctuations in temperature, pressure, humidity, etc. As we will discuss below, all of these alternatives remain viable at present.

The suggestion that the decay parameter λ may be time-dependent derives not only from the BNL, PTB, and solar flare data cited above (and discussed below), but also from a number of earlier experiments which are summarized in Table 1. In addition to the experiments cited there, which report direct evidence for time-varying decay parameters, there may be indirect indications of varying decay parameters if one takes seriously apparent discrepancies arising from half-life determinations of some nuclides by different groups. Although it would be reasonable to attribute these discrepancies to unspecified systematic effects, the possibility that these arise from a common source is suggested by the fact that many such discrepancies are cited in the literature in experiments carried out by experienced, well-

known groups (Alburger et al. 1986; Begemann et al. 2001; Chiu et al. 2007; Pommé 2007; Pommé et al. 2008).

We conclude by outlining the present paper. As noted above, Sect. 2 contains the discussion of the BNL and PTB correlations, and Sect. 3 presents the data from the solar flare of 2006 December 13. In Sect. 4 we develop the phenomenology of a time-varying decay parameter $\lambda(t)$, and discuss some experimental implications. One of the main objectives of the present paper is to discuss possible mechanisms through which solar activity could affect nuclear decays, and this discussion for β-decays is presented in Sect. 5, along with a discussion of the relevant β-decay phenomenology. This section also discusses some of the constraints on mechanisms which aim to explain the data in Sects. 2 and 3 in terms of new interactions. In Sect. 6 we present a brief discussion of constraints on possible mechanisms to explain time-varying decay parameters in α-decay. Following the appearance of our original papers on the BNL/PTB data (Jenkins et al. 2008), and on the solar flare data (Jenkins and Fischbach 2008), additional data came to light which both questioned and supported our results, and these are discussed in Sect. 7. In Sect. 8 we comment on the implications of this work to ^{14}C dating. In Sect. 9 we present a summary of present and future experiments testing the constancy of nuclear decay parameters, and in Sect. 10 we discuss the implications of this work for possibly detecting the relic neutrino background. We conclude by summarizing our results in Sect. 11.

2 Evidence for Correlations Between Nuclear Decay Rates and Earth–Sun Distance

As noted in the Introduction, our interest in the possibility that nuclear decay parameters λ might vary with time arose from an unrelated effort to apply a new randomness test (Tu and Fischbach 2003, 2005) to nuclear decays. This effort eventually led us to a number of interesting data sets which indicated an apparent time-dependence of λ, most notably the BNL data of Alburger et al. (1986), and the PTB data of Siegert et al. (1998), Schrader (2008). (We note that a time-dependence of λ does not necessarily imply any deviation from randomness, but only a deviation in the probability distribution which governs the decays.) In this Section we present a summary and analysis of these two data sets.

Between 1982 and 1986, Alburger et al. (1986) measured the half-life of ^{32}Si at BNL via a direct measurement of the counting rate as a function of time. As is typical in such counting experiments, the counting rate for ^{32}Si was continually monitored in the same detector against a long-lived comparison standard, which in the BNL experiment was ^{36}Cl ($T_{1/2} = 301{,}000$ y). Counts were taken with a precision sample changer (Harbottle et al. 1973), where each of the ^{32}Si and ^{36}Cl sources was counted for 30 minutes alternately, 10 times each. The 10 counts were then summed for each source, and the ^{32}Si/^{36}Cl ratio was generated. Three days of counting were done for each reported week, and all of the data points were used in our analysis. Since the fractional change in the ^{36}Cl counting rate over the four year duration of the experiment was only $\mathcal{O}(10^{-5})$, which was considerably smaller than the overall uncertainty of the final result, $T_{1/2}(^{32}\mathrm{Si}) = 172(4)$ y, the ^{36}Cl decay rate was assumed to be constant. Any time dependence for ^{36}Cl beyond the expected statistical fluctuations was then presumed to arise from various systematic effects, such as drift in the electronics. By computing the ratio $^{32}\mathrm{Si}/^{36}\mathrm{Cl} \equiv \dot{N}(^{32}\mathrm{Si})/\dot{N}(^{36}\mathrm{Cl})$, these apparatus-dependent systematic effects should have largely cancelled (see discussion below), and hence this ratio was used to obtain the half-life of ^{32}Si.

If there was any residual unexpected behavior of the ratio ^{32}Si/^{36}Cl, one would naturally seek to explain this behavior in terms of the differential response of the two nuclides' individual measured counting rates to possible variations in the measuring apparatus. If such

an explanation did not quantitatively explain the anomalous residual behavior, one could then reasonably consider the possibility that the residual unexpected behavior was in fact due to variations in the individual decay parameters themselves. Since we generally expect different nuclides to exhibit different time-dependent fractional variations, it follows that such an effect could account for any residual unexplained behavior in the ratio ^{32}Si/^{36}Cl. We note, however, that two different nuclides might indeed experience similar variations in their intrinsic decay parameters, perhaps as a consequence of the details of the mechanism, or perhaps just by chance. Hence, the failure to see any unexpected behavior in the ratio of the nuclides' count-rates does not necessarily imply that the interesting behavior of the nuclides individually is entirely due to systematic effects in the measuring apparatus. As such, if the behavior of the nuclides' individual measured counting rates seems difficult to explain in terms of systematic effects of the apparatus, one could tentatively consider the possibility that the experiment is suggesting an intrinsic variation in individual decay parameters. This latter comment will be seen to be relevent to the PTB data, to be discussed shortly.

The BNL data for the ratio ^{32}Si/^{36}Cl revealed an unexpected annual variation which led Alburger et al. (1986) to study the sensitivity of their detection system to changes in various experimental parameters, including counter voltage and gas flow, box pressure and temperature, and discriminator level. In addition, backgrounds were measured and found to be negligible. In the end, Alburger et al. (1986) concluded that "...systematic periodic variations are present but that they cannot be fully accounted for by our tests or estimates."

Since several annually varying effects happen to closely track the varying distance R between the Earth and the Sun (e.g. local temperatures), it is reasonable to ask whether the BNL data correlate directly with either $1/R^2$ or $1/R$ (we note that our existing data cannot distinguish between these two possibilities). When comparing the results from experiments on different nuclides, it is convenient to study the function $U(t) \equiv [\dot{N}(t)/\dot{N}(0)]\exp(+\lambda t)$ rather than $\dot{N}(t)$ itself, since $U(t)$ should be time-independent for all nuclides. For ^{32}Si, we used $\lambda = 4.0299 \times 10^{-3}$ y^{-1} from Alburger et al. (1986). Figure 1 exhibits $U(t)$ for the ^{32}Si/^{36}Cl BNL data, along with a plot of $1/R^2$. An annual modulation of the ^{32}Si/^{36}Cl ratio is clearly evident, as was first reported in Alburger et al. (1986). The Pearson correlation coefficient, r (Taylor 1997, p. 217), between the raw BNL data and $1/R^2$ (or $1/R$) is $r = 0.52$ for $N = 239$ data points, which translates to a formal probability of 6×10^{-18} that this correlation would arise from two data sets which were uncorrelated. There is also a suggestion in Fig. 1 of a phase shift between $1/R^2$ and the BNL data, which we discuss in greater detail below.

The annual variation observed in the BNL decay data raised the question of whether similar effects could be present in other decays as well. Although there are hundreds of potentially useful nuclides whose half-lives have been measured, the data from many of the experiments we examined were generally not useful, most often because data were not acquired continuously over sufficiently long time periods. However, we were able to obtain the raw data from an experiment carried out at the PTB in Germany (Schrader 2008; Siegert et al. 1998) measuring the half-lives for ^{152}Eu and ^{154}Eu, in which ^{226}Ra was the long-lived comparison standard. The data were collected with a high-pressure $4\pi\gamma$ ionization chamber, measured as a current, and each measurement was corrected for background, as described by the PTB experimental protocol: "The ionization chamber was equipped with an automated sample changer that allowed the sources under study, background, and a radium reference source to be successively measured" (Schrader 2008; Siegert et al. 1998). Each data point in Fig. 2 is then an average of approximately 30 individual measurements of the ^{226}Ra current corrected for background. The contribution to the ^{226}Ra counting rate from such background radiation as ^{222}Rn, which is known to fluctuate seasonally (Wissman 2006), is subtracted

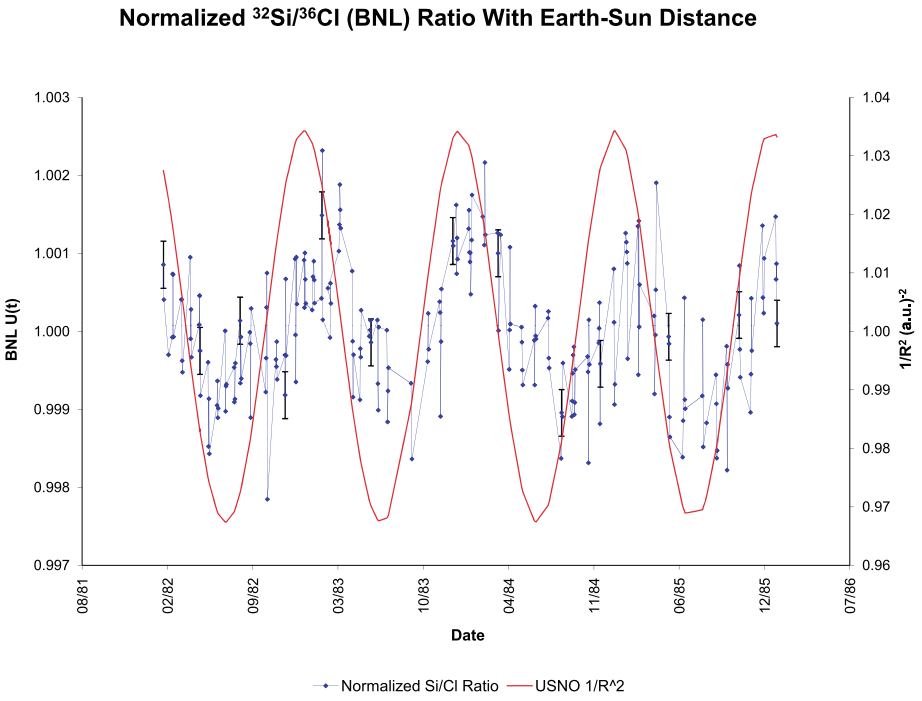

Fig. 1 Plot of $U(t)$ for the raw BNL ^{32}Si/^{36}Cl ratio along with $1/R^2$ where R is the Earth–Sun distance. $U(t)$ is obtained by multiplying each data point by $\exp(+\lambda t)$ where $\lambda = \ln(2)/T_{1/2}$ and $T_{1/2} = 172$ y for ^{32}Si. The *left axis* gives the scale for the normalized $U(t)$, and the *right axis* denotes the values of $1/R^2$ in units of $1/(\text{a.u.})^2$ obtained from the U.S. Naval Observatory (USNO). The fractional change in ^{32}Si counting rates between perihelion and aphelion is approximately 3×10^{-3}. As noted in the text, the correlation coefficient between the BNL data and $1/R^2$ (or $1/R$) is $r = 0.52$ for $N = 239$ points. The formal probability that the indicated correlation could have arisen from uncorrelated data sets is 6×10^{-18}

out for each individual data point, thus suppressing any seasonal contribution. The same subtraction applies to other potential backgrounds, such as cosmic rays. Other environmental factors such as ambient temperature, pressure, and relative humidity would lie within what is typical for a laboratory environment, and are not expected to have a significant effect on the detection system. Any changes within the normal laboratory setting, however, should be mitigated by the fact that the system was a high-pressure (2 MPa) ionization chamber, detecting photons traversing a very short range within the $4\pi\gamma$ setup. The PTB experiment, which extended over 15 years, exhibited annual fluctuations in the ^{226}Ra data similar to those seen at BNL.

We note that the data plotted in Fig. 2 are the raw ^{226}Ra data rather than the ratio ^{152}Eu/^{226}Ra as might be expected from an analogy to Fig. 1. There are two reasons for this: (a) In contrast to the BNL data, where we were given copies of the original notebooks containing the raw ^{32}Si and ^{36}Cl data, in the PTB case the data we received had already been processed in a way that would have been difficult for us to undo. (b) Secondly, ^{152}Eu is an interesting nuclide for present purposes because it decays by both electron capture (72%) and β-decay (28%). Since these two decay modes could very well exhibit different time-dependent responses to a given external perturbation, the time-dependence of ^{152}Eu could be more complicated than that of the other nuclides whose data we have analyzed.

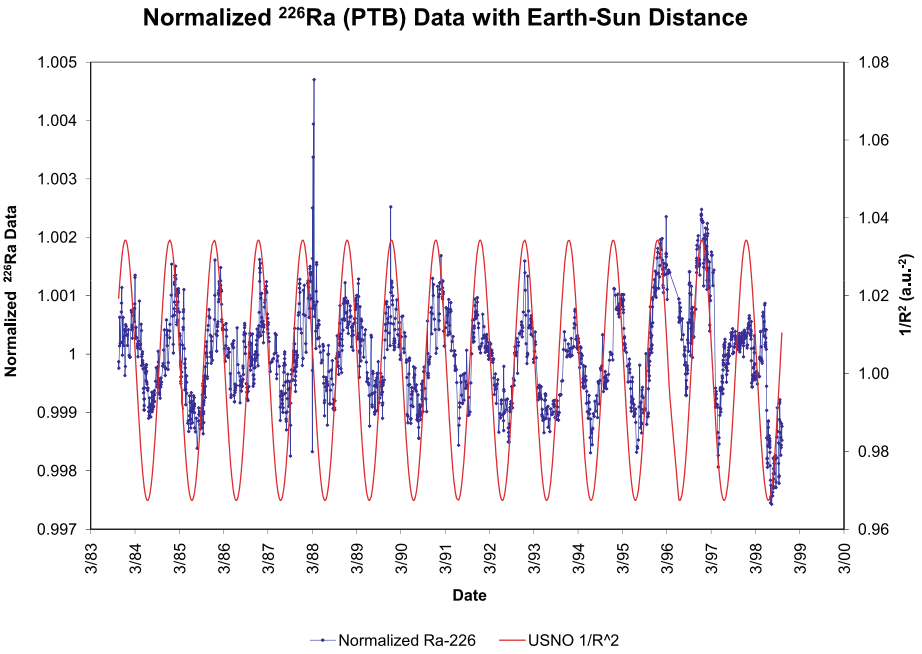

Fig. 2 Plot of $U(t)$ for the raw PTB ^{226}Ra data (using $T_{1/2} = 1600$ y) along with $1/R^2$. As noted in the text, the correlation coefficient between the PTB data and $1/R^2$ is $r = 0.62$ for $N = 1974$ points. The formal probability that the indicated correlation could have arisen from uncorrelated data sets is 5×10^{-210}. See caption to Fig. 1 for additional details

As in the case of the BNL data, it is again reasonable to ask whether these data correlate with $1/R^2$. The Pearson correlation coefficient r for the data in Fig. 2 is $r = 0.62$ for $N = 1974$ data points corresponding to a formal probability of 5×10^{-210} that the two data sets were in fact uncorrelated. There is also a suggestion of a phase shift between $1/R^2$ and the PTB data, as in the BNL data.

Given that the BNL and PTB experiments overlapped for ∼2 years, we can also calculate the correlation coefficient between the BNL and PTB data. For the weeks during which the BNL and PTB data sets had concurrent measurements, averages for each week's measurements (the ^{32}Si/^{36}Cl ratios for BNL and the currents for PTB) were taken in each data set in order to maintain consistency, and the resulting correlation is exhibited in Figs. 3 and 4. The Pearson correlation coefficient for the raw BNL and PTB data is $r = 0.66$ for $N = 39$ points, which corresponds to a formal probability of 6×10^{-6} that this correlation could have arisen from two uncorrelated data sets.

Notwithstanding the possible implications of the correlations between the BNL and PTB data, some words of caution are appropriate relating to our use of the ^{226}Ra data. When the ratio is taken between the counts of ^{154}Eu and ^{226}Ra, a periodic signal is no longer evident (see Fig. 3 in Siegert et al. 1998), in contrast to what is seen in the BNL data. Referring to the previous discussion, the absence of a periodic signal in the ^{154}Eu/^{226}Ra ratio could be attributed to a similar response of the individual ^{154}Eu and ^{226}Ra count-rates to a variation in the measuring apparatus. We note that, unlike the PTB europium data, the ^{226}Ra data we have analyzed are raw data, having no corrections other than background subtraction. It would thus appear that the periodic signal present in the ^{226}Ra data is either a manifestation

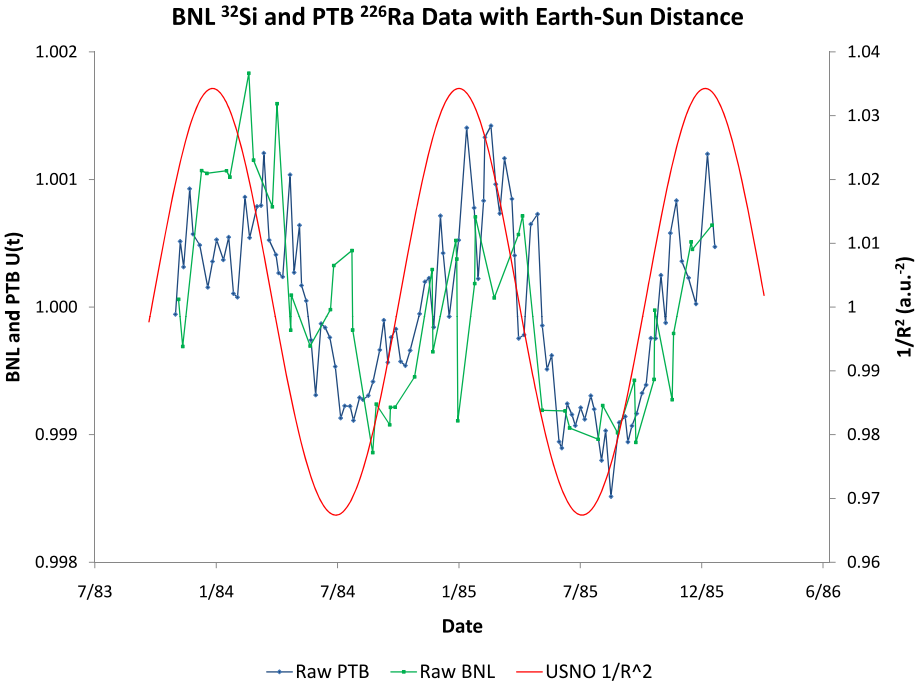

Fig. 3 Correlation between the raw decay rates of ^{32}Si/^{36}Cl at BNL and ^{226}Ra at PTB. The BNL and PTB data for $U(t)$ have been averaged in common weekly bins for purposes of comparison. The correlation coefficient between the BNL and PTB data is $r = 0.66$ for $N = 39$ points, which corresponds to a probability of 6×10^{-6} that the BNL/PTB correlation could have arisen from uncorrelated data sets as a result of statistical fluctuation. *Error bars* are shown for representative BNL data points, and the *error bars* for the PTB data lie within the points themselves

of fluctuations arising from the measuring apparatus, or else results from fluctuations in the ^{226}Ra decay parameter itself. One would naturally seek to ascertain whether any variations in the measuring instrumentation would be capable of producing the observed periodic signal in the ^{226}Ra data. Siegert et al. (1998) have proposed a qualitative mechanism whereby background radioactivity due to radon and daughter products could affect the apparatus, but no quantitative analysis was given. It therefore seems reasonable to regard the origin of the periodic signal in the ^{226}Ra measured count-rate as an open question, and we have thus suggested the possibility that the PTB data are indicating variations in the decay parameters of ^{226}Ra or its daughters. This seems to imply that the fractional variations in the decay parameters of ^{154}Eu and ^{226}Ra are very similar, which one generally would not expect, and this could be a clue to the nature of a possible physical mechanism.

The correlations of the BNL and PTB data with $1/R^2$, as well as with each other, do not in and of themselves point to an origin for these effects. Not only are there several potential influences which could depend on R, but additionally there are seasonal variations that roughly track with R even though the Earth–Sun distance is not their primary cause (e.g. local temperature variations). Having previously addressed the possibility that these correlations arise from seasonal fluctuations in the detectors used in the BNL and PTB experiments, we next consider the possibility that the time-dependence of the ^{32}Si/^{36}Cl ratio and the ^{226}Ra decay rate are being modulated by an annually varying flux or field originating

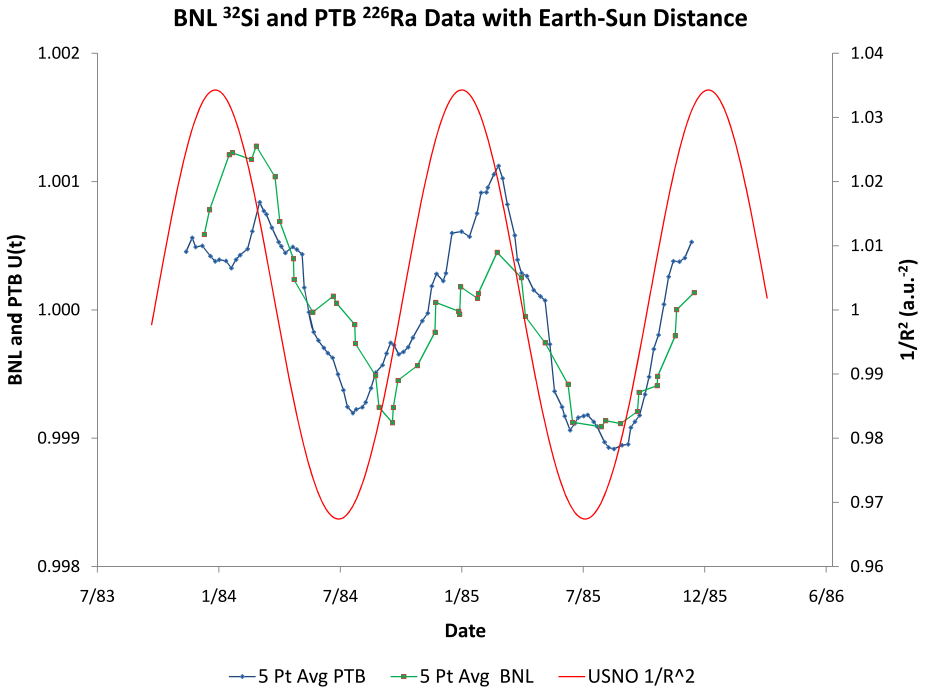

Fig. 4 Correlation between the centered 5 point averaged decay rates of ^{32}Si/^{36}Cl at BNL and ^{226}Ra at PTB. The centered 5 point average illustrates the effect of smoothing out short-term fluctuations in both data sets. The BNL and PTB data for $U(t)$ have been averaged in common weekly bins for purposes of comparison

from the Sun. The fact that the two decay processes are very different (α-decay for ^{226}Ra and β-decay for ^{32}Si) would seem to preclude a common mechanism for both. We note, however, that even though ^{226}Ra decays via α-emission, its daughter products include ^{214}Bi and ^{214}Pb, which are β-decays and which rapidly reach equilibrium with the parent ^{226}Ra (see Sect. 7 below). It is thus possible that a single mechanism could explain the ^{32}Si and ^{226}Ra data, provided that its dominant effects appeared in the β-decays. However, there are also mechanisms which could affect both β- and α-decays, such as proposed in the recent papers by Barrow and Shaw (Barrow and Shaw 2008; Shaw 2007) which we discuss in more detail in Sect. 6 below.

Returning to Figs. 1–4, we briefly explore the suggestion noted above of a possible phase shift of $1/R^2$ relative to both the BNL and PTB data. One possibility could be additional contributions to periodic variations in neutrino flux, which might arise from a small neutrino magnetic dipole moment. Sturrock (2008) has recently shown that data on solar neutrino flux and solar irradiance exhibit a common modulation at 11.85 y^{-1} (period = 31 d), which is thought to arise from the rotation of the solar core. It is thus possible that the ~1 month phase lag evident in Figs. 1–4 could be related in some way to Sturrock's observations, although this would require more than a simple superposition of a monthly and an annual sine curve. Yet another possibility for the apparent phase shift is that the effect depends on the Earth's velocity relative to some fixed direction in space. Such an effect might share similarities with the mechanism proposed by the DAMA/LIBRA collaboration (Bernabei et al. 2008), though we note that their particular model involves the Earth's motion through the galactic rest frame, and would thus be roughly 2 months out of phase with the BNL/PTB

data. However, we note in passing that the superposition of two annually varying periodic effects of comparable strength, one of which is in phase with $1/R^2$, and the other with our speed through the galactic rest frame, could give rise to a phase shift of ~ 30 days, as present in the BNL/PTB data.

3 Implications of the Solar Flare of 2006 December 13

As noted in the Introduction, data taken during the solar flare of 2009 December 13 lend support to the inference from the BNL and PTB data that solar activity can influence nuclear decay rates. In this Section we summarize this experiment and refer the reader to Jenkins and Fischbach (2008) for a more detailed discussion.

The apparatus that was in operation during the solar flare was a $\sim$1 μCi sample of ^{54}Mn attached to the front of a Bicron 2 × 2 inch NaI(Tl) crystal detector, which was connected to an Ortec photomultiplier (PMT) base with pre-amplifier. An Ortec 276 spectroscopy amplifier was used to analyze the pre-amplifier signal, and this was connected to an Ortec Trump® PCI card running Ortec's Maestro32® MCA software. The system recorded the 834.8 keV γ-ray emitted from the de-excitation of ^{54}Cr produced from the electron-capture process $^{54}\mathrm{Mn} + e^- \rightarrow {}^{54}\mathrm{Cr} + \nu_e$. The detector and the ^{54}Mn sample were shielded on all sides by several inches of lead, except at the end of the PMT base where a space was left to accommodate cables. The apparatus was located in a windowless, air-conditioned interior 1st floor room in the Physics building at Purdue in which the temperature was maintained at a constant 19.5(5)°C.

During the course of the data collection, which extended from 2006 December 2 to 2007 January 2, a solar flare was detected on 2006 December 13 at 02:37 UT (21:37 EST on December 12) by the Geostationary Operational Environmental Satellites (GOES-10 and GOES-11). Spikes in the X-ray and particle fluxes were recorded on all of the GOES satellites (NOAA 2009) during the course of the four days following the initial flare on December 13. The X-ray data from this X-3 class solar flare are shown in Figs. 5 and 6 along with the ^{54}Mn counting rates: in each 4 hour live-time period ($\sim$4.25 hours real-time) we recorded $\sim 2.5 \times 10^7$ counts of 834.8 keV γ-rays with a fractional $1/\sqrt{N}$ statistical uncertainty of $\sim 2 \times 10^{-4}$. Each ^{54}Mn data point in Figs. 5 and 6 then represents the number of counts in the subsequent 4 hour period, which are normalized in Fig. 6 by the number of counts $N(t)$ expected from a monotonic exponential decay $N(t) = N_0 \exp(-\lambda t)$, with $\lambda = 0.002347(2)$ d^{-1} determined from our December data. We see from Figs. 5 and 6 that, to within the time resolution offered by the 4 hour width of our bins, the ^{54}Mn count rates exhibit a dip which is coincident in time with the spike in the X-ray flux which signalled the onset of the solar flare. Although a second X-ray peak on December 14 at 17:15 EST corresponds to a relatively small dip in the ^{54}Mn count-rate, a third peak on December 17 at 12:40 EST is again accompanied by an obvious dip in the ^{54}Mn counting rate, as seen in Figs. 5 and 6. The fact that some X-ray spikes in these and other data sets are not accompanied by correspondingly prominent dips in the ^{54}Mn data may provide clues to the underlying mechanisms that produce these solar events. Additionally, the X-ray flare that occurred earlier in the month on December 5 was not Earth-directed, which may explain the relatively small change in the observed ^{54}Mn count-rate. Conversely, peaks or dips in the ^{54}Mn data not accompanied by visible X-ray spikes may correspond to other types of solar events, or to events on the opposite side of the Sun, which are possibly being detected via neutrinos. In particular, the dip on 2006 December 22 (09:04 EST) was coincident in time with a severe solar storm (NOAA 2006), but did not have an associated X-ray spike.

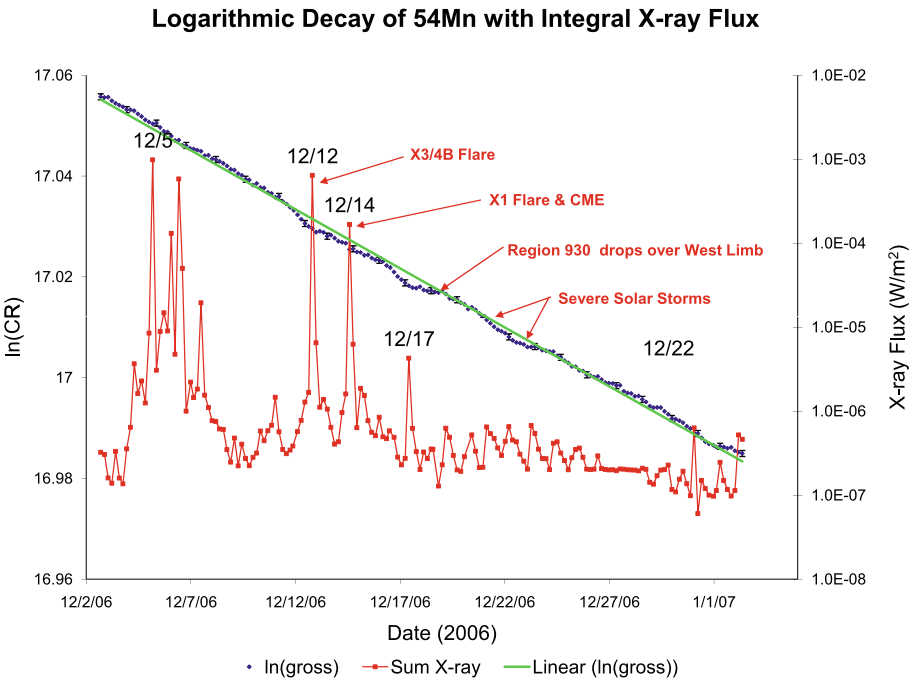

Fig. 5 December 2006 ^{54}Mn data, and GOES-11 X-ray data, both plotted on a logarithmic scale. For ^{54}Mn, each point represents the natural logarithm of the number of counts $\sim 2.5 \times 10^7$ in the subsequent 4 hour period, and has a $3 \times 1/\sqrt{N}$ statistical error shown by the indicated (small) error bars. For the GOES-11 X-ray data, each point is the solar X-ray flux in W/m^2 summed over the same real time intervals as the corresponding decay data. The *solid line* is a fit to the ^{54}Mn data, and deviations from this line coincident with the X-ray spikes are clearly visible on 12/12 and 12/17. As noted in the text, the deviation on 12/22 was coincident with a severe solar storm, with no associated flare activity (NOAA 2009). The dates for other solar events are also shown by *arrows*

Before considering more detailed arguments supporting our inference that the ^{54}Mn count-rate dips are due to changes in the flux of solar neutrinos, we address the question of whether the coincident fluctuations in the decay data and the solar flare data could simply arise from statistical fluctuations in each data set. Referring to Fig. 5, we define the dip region in the decay data as the 84 hour period (encompassing our runs 51–71 inclusive) extending between 2006 December 11 (17:52 EST) and 2006 December 15 (06:59 EST). The measured number of decays N_m in this region can then be compared to the number of events N_e expected in the absence of the observed fluctuations, assuming a monotonic exponential decrease in the counting rate. Since the systematic errors in N_e and N_m are small compared to the statistical uncertainties in each, only the latter are retained and we find

$$N_e - N_m = (7.51 \pm 1.07) \times 10^5, \tag{1}$$

where the dominant contributions to the overall uncertainty arise from the $\sqrt{N}$ fluctuations in the counting rates. If we interpret (1) in the conventional manner as a $\sim 7\sigma$ effect, then the formal probability of such a statistical fluctuation in this 84 hour period is $\sim 3 \times 10^{-12}$. This conclusion is not altered by including additional small systematic corrections.

We next estimate the probability that a solar flare would have occurred during the same 84 hour period shown in Fig. 5. The frequency of solar radiation storms varies with their

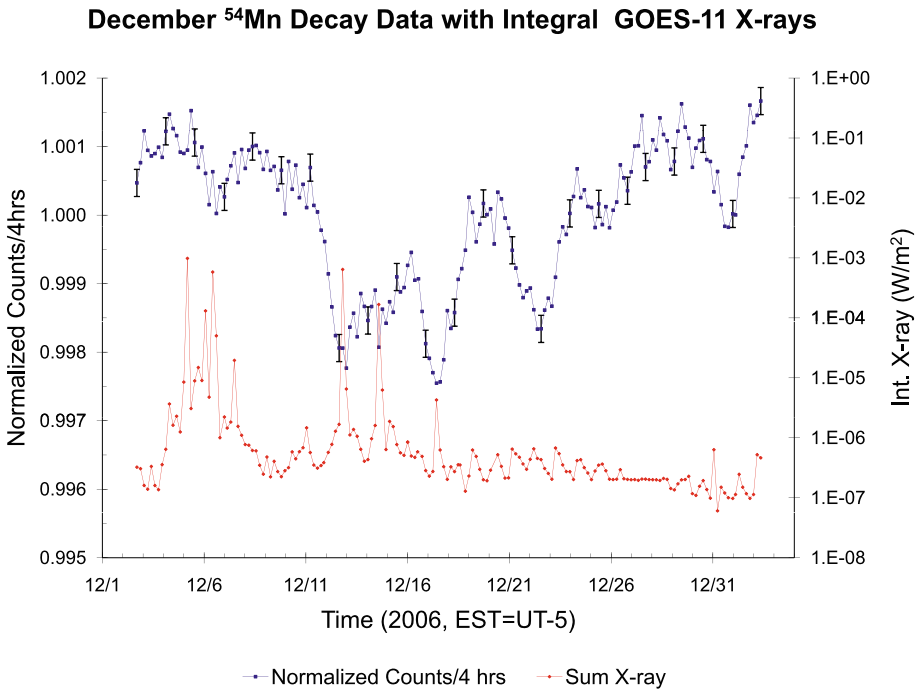

Fig. 6 Normalized December 2006 ^{54}Mn decay data along with GOES-11 X-ray data on a logarithmic scale. For ^{54}Mn, each point represents the number of counts in the subsequent four hour period normalized to the average decay rate (see text), and has a fractional $1/\sqrt{N}$ statistical uncertainty of $\sim 2 \times 10^{-4}$. For the GOES-11 X-ray data, each point is the solar flux in W/m^2 summed over the same real-time intervals. The 2006 December 12 spike in solar flux occurred at $\sim$21:37 EST

intensities, which are rated on a scale from S1(Minor) to S5(Extreme) (NOAA 2005). The 2006 December 13 event was rated as S2 (Moderate), and S2 storms occur with an average frequency of 25 per 11 year solar cycle (NOAA 2009). In total, the frequency of storms with intensity $\geq$S2 is $\sim$39 per 11 year solar cycle, or 9.7×10^{-3} d^{-1}, and hence the probability of a storm occurring at any time during the 84 hour window in Fig. 5 is $\sim 3.4 \times 10^{-2}$. Evidently, if the X-ray and decay peaks were uncorrelated, the probability that they would happen to coincide as they do over the short time interval of the solar flare would be smaller still, and hence a conservative upper bound on such a statistical coincidence occurring in any 84 hour period is $\sim (3 \times 10^{-12})(3 \times 10^{-2}) = 1 \times 10^{-13}$. Since a similar analysis would apply to the coincident peak and dip at 12:40 EST on December 17, the probability that random fluctuations would produce two sets of coincidences several days apart is negligibly small, and hence we turn to consider other possible explanations for the data in Figs. 5 and 6.

Solar flares are known to produce a variety of electromagnetic effects on Earth, including changes in the Earth's magnetic field, and power surges in the electric grids. It is thus conceivable that the observed dips in the ^{54}Mn counting rate could have arisen from the response of our detection system (rather than the ^{54}Mn atoms themselves) to the solar flare. The most compelling argument against this explanation of the ^{54}Mn data is that the ^{54}Mn decay rate began to decrease more than one day *before* any signal was detected in X-rays by the GOES satellites (see Figs. 5 and 6 in text). Since it is unlikely that any other electromagnetic signal would reach the Earth earlier than the X-rays, we can reasonably exclude any explanation of

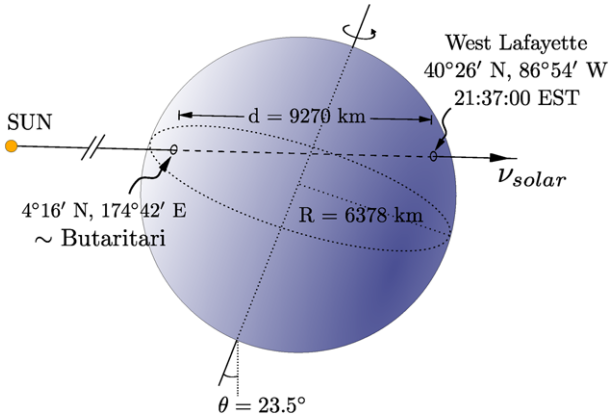

Fig. 7 Trajectory of neutrinos from the solar flare of 2006 December 12 21:37 EST. The neutrinos would have entered the Earth near Butaritari, in the Pacific Ocean, and travelled ∼9270 km through the Earth before the coincident minimum in the count-rate was detected in West Lafayette, Indiana

the ^{54}Mn data in terms of a conventional electromagnetic effect arising from the solar flare. This is particularly true since the most significant impact on the geomagnetic field occurs with the arrival of the charged particle flux, several hours after the arrival of the X-rays. Figure 8 exhibits the A_p index for the Earth's magnetic field during 2006 December,[1] along with the ^{54}Mn counting rate. We see immediately that the sharp spike in the A_p index at approximately 00:00 EST on 2006 December 15 occurred more than two days *after* the solar flare and the accompanying dip in the ^{54}Mn counting rate, and hence was presumably not the cause of this dip. This conclusion was further strengthened by the results of a series of measurements carried out in our laboratory, which established that our detection system was insensitive to applied magnetic fields that were more than 100 times stronger than the spike exhibited in Fig. 8.

The response of our detection system to fluctuations in line voltages was also studied. No unusual behavior was detected by either the Purdue power plant, or by the Midwest Independent Systems Operator (MISO) which also supplies power to Purdue. MISO did in fact receive notification on 14 December 2006 of a "Geo-magnetic disturbance of K-7 magnitude" at 02:46 UT, but noted that there were no reported occurrences of excessive neutral currents during the time-frame of 10–18 December 2006. At Purdue, an alert would have been triggered had the line voltage strayed out of the range 115–126 V, and hence we can infer that the voltage remained within this range during the solar flare. Moreover, since the main effect of a power surge would have been to shift the ^{54}Mn peak slightly out of the nominal region of interest (ROI) for the 834.8 keV γ-ray, this would have been noted and corrected for in the routine course of our data acquisition. No significant changes to either the peak shape or location were noted during this period. Additional post-experiment testing showed that the line voltage at Purdue is confined to the range 120 ± 5 V, and within this range, no apparent effects were seen in similar counting experiments.

We therefore turn to the possibility that this dip was a response to a change in the flux of solar neutrinos during the flare, as implied by the analysis of Jenkins et al. (2008). To begin we note that the X-ray spike coincident with the maximum deviation of the ^{54}Mn count-rate from the expected rate occurred at ∼21:40 EST, approximately 4 hours after local sunset, which was at ∼17:21 EST on 2006 December 12. As can be seen from Fig. 7, the neutrinos (or whatever other agent produced this dip) had to travel ∼9,270 km through the Earth

[1] http://www.swpc.noaa.gov.

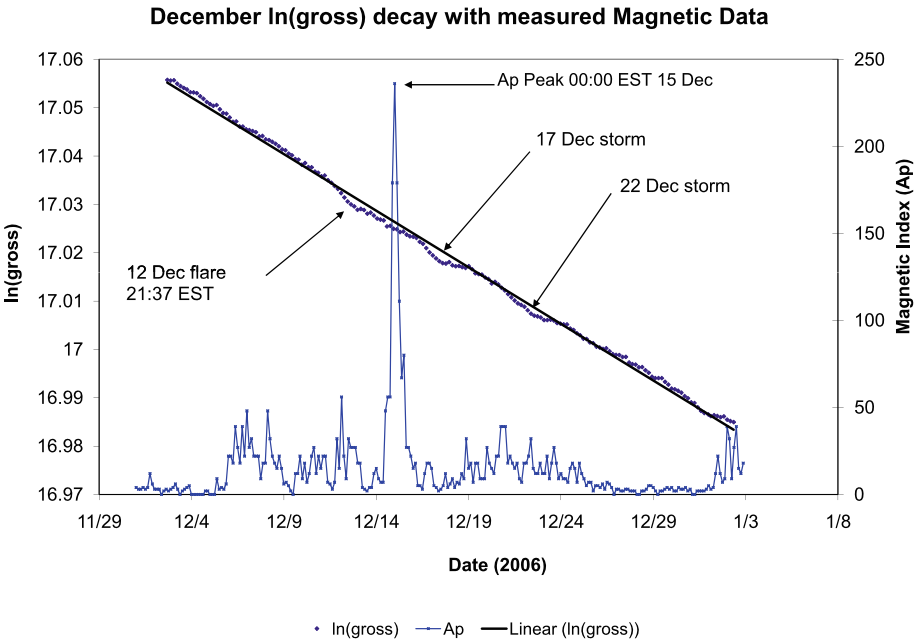

Fig. 8 Fluctuations in the Earth's magnetic field in December 2006. The magnetic field fluctuations, which are characterized by the A_p index, are plotted along with the natural logarithm of the ^{54}Mn count-rate. We note that the spike in the magnetic data on 2006 December 15 occurred ∼2 days *after* the dip in the ^{54}Mn count-rate at 21:37 EST on 2006 December 12

before reaching the ^{54}Mn source, and yet produced a dip in the counting rate coincident in time with the peak of the X-ray burst. Significantly, the monotonic decline of the counting rate in the 40 hours preceding the dip occurred while the Earth went through 1.7 revolutions, and yet there are no obvious diurnal or other periodic effects. These observations support our inference that this effect may have arisen from neutrinos, some neutrino-like particles, or some field emanating from the Sun, and not from any conventionally known electromagnetic effect or other source, such as known charged particles.

4 Phenomenology of a Time-Dependent Decay Parameter $\lambda(t)$

As noted in the previous sections, one implication of the BNL/PTB data correlations and the solar flare data is that nuclear decay parameters may be influenced by the external environment, and hence may not actually be constant. In this section we outline some of the phenomenological implications of a decay parameter $\lambda = \lambda(t)$ which is time-dependent.

If $P(t)$ denotes the probability that a nucleus has not decayed after a time t, then the probability that it has still not decayed after a time $(t + dt)$ is given by

$$P(t + dt) = P(t)[1 - \lambda(t)dt]. \tag{2}$$

In (2) $\lambda(t)dt$ is the probability of decay in the time interval t to $(t + dt)$ and hence $[1 - \lambda(t)dt]$ is the corresponding survival probability. Rearranging (2) we have

$$\dot{P}(t) = \frac{P(t + dt) - P(t)}{dt} = -\lambda(t)P(t), \tag{3}$$

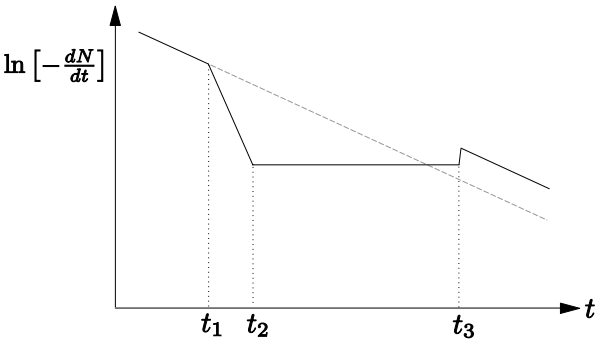

Fig. 9 Schematic illustration of a flat region in the decay curve. As shown in Fig. 10 flat regions are seen experimentally in the ^{54}Mn data. See text for additional details

and integrating (3) we find

$$P(t) = P(0)\exp\left[-\int_0^t dt'\lambda(t')\right]. \tag{4}$$

When $\lambda(t)$ is time-independent $P(t)$ reduces to the familiar exponential decay law with $P(0)$ set to unity. For a sample of N_0 atoms at $t = 0$ experiencing a common external interaction, the number $N(t)$ surviving at a time t is then given by

$$N(t) = N_0\exp\left[-\int_0^t dt'\lambda(t')\right]. \tag{5}$$

In principle one can extract from (5) a wide range of expressions for $N(t)$ by an appropriate choice of $\lambda(t)$. Any "anomalous slope region", i.e. a deviation of the experimental data for $N(t)$ and $dN(t)/dt$ from the expected forms (with constant λ)

$$N(t) = N_0 e^{-\lambda t}, \qquad \frac{dN}{dt} = -\lambda N_0 e^{-\lambda t}, \tag{6}$$

could then be taken as evidence that λ is itself time-dependent. Among the possible functional dependencies for $\lambda(t)$ that one might consider, two are of special interest, since they lead to variations in dN/dt that are suggested by existing data. One is a sinusoidal variation of dN/dt as we have already discussed in Sect. 2. The other is a "flat region", which is an extended period of time during which dN/dt remains approximately constant, notwithstanding the depletion of the sample population. Although in principle a "flat region" is no more fundamental than any other deviation from the expected behavior of dN/dt, it is both visually striking and straightforward to describe. In what follows we consider this case first, and discuss some potential medical implications of anomalous slope regions.

To see how we may obtain a flat region mathematically, we start with (5) and, taking a derivative, we find

$$\frac{dN}{dt} = -N_0\lambda(t)\exp\left[-\int_0^t \lambda(t')dt'\right] \cong -N_0\lambda(t)\cdot\left[1-\int_0^t \lambda(t')dt'\right], \tag{7}$$

where we have assumed that t is sufficiently small that the exponent may be expanded to lowest order. It is straightforward to show that if

$$\lambda(t) = \frac{\lambda(0)}{\sqrt{1-2\lambda(0)t}}, \tag{8}$$

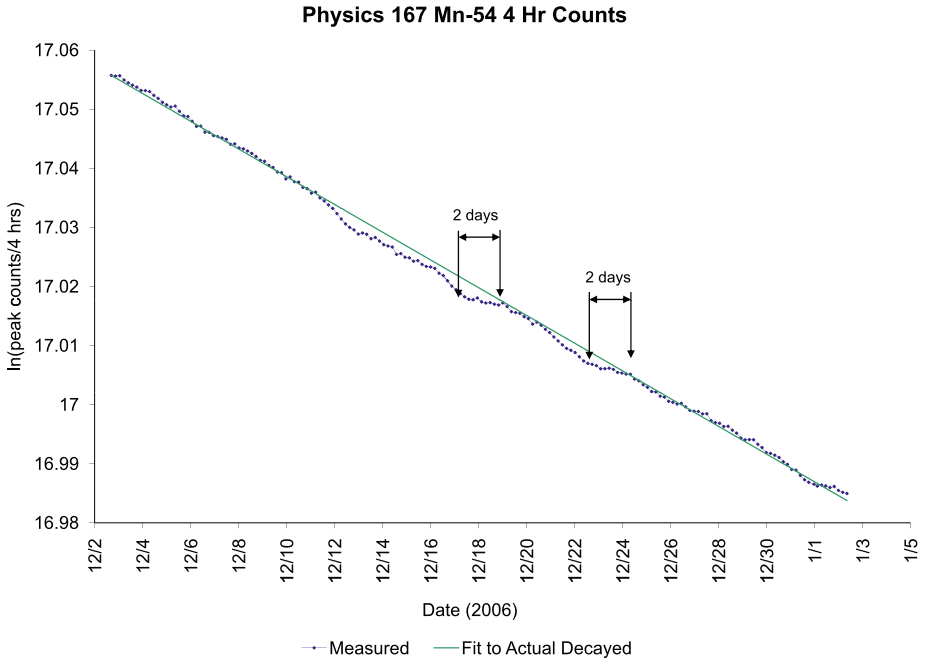

Fig. 10 Flat regions in the Purdue ^{54}Mn decay data. During the periods shown the count-rates were approximately constant

then (8) gives a flat region with constant decay-rate given by $N_0\lambda(0)$ when $\lambda(0)t \ll 1$. One can see in this way that (7) can produce a decay curve of basically any shape, given the appropriate $\lambda(t)$, though in the general case it may be difficult to find analytic forms for $\lambda(t)$. One can also write $\lambda(t)$ as a power series, which is valid for larger values of $\lambda(0)t$, by writing

$$\lambda(t) = \lambda(0) + \sum_{n=1}^{\infty} \lambda_n t^n, \tag{9}$$

where λ_n are appropriate dimensional constants. Setting $\lambda_n = \lambda^{n+1}(0)$ eliminates the t-dependence in dN/dt through $\mathcal{O}[(\lambda(0)t)^n]$, and hence creates a "flat region" of this order. The leading t-dependent term is then $\lambda_1 t = \lambda^2(0)t$, in agreement with (8). We note from (8) that $\lambda(t)$ is an increasing function of t as we expect on physical grounds: since the number of atoms $N(t)$ available to decay is always a decreasing function of time, the only way for the actual decay-rate $|dN/dt|$ to remain approximately constant is if the effect of decreasing $N(t)$ is offset by an increasing $\lambda(t)$. As we note from Fig. 10, regions where $dN/dt \sim$ constant are seen in the ^{54}Mn data we have taken at Purdue. (There are also suggestions of flat regions in the ^{152}Eu data from PTB.)

Returning to Fig. 9 we describe what is happening physically in the different time intervals as follows: at t_1 the decay parameter begins to decrease, and therefore so does the decay rate $|dN/dt|$. At t_2 the decay parameter $\lambda(t)$ starts to increase in such a way that the decay rate remains constant. By t_3, the decay parameter has increased back to its original value $\lambda(t_1)$ and thereafter remains constant. Note that the specified variation in λ implies

that a larger population of active nuclei remains at t_3 compared to what would have been expected from an extrapolation of the original trend curve. Moreover, since λ has reverted to its original value, we see that the decay curve for $t > t_3$ is parallel to the extrapolated curve, but displaced upward. (A different fluctuation in λ could result in the curve being displaced downward.) Figure 9 illustrates the case for ^{54}Mn where $\lambda(t) \to \lambda(t < t_1)$ instantaneously at t_3. For the ^{54}Mn data taken during the 2006 December 13 flare we estimate that the fractional shift in the counting rate after the flare was $\mathcal{O}(10^{-5})$, which is too small an effect for us to have detected as a shift of the decay curve.

It should be emphasized that the above discussion is somewhat schematic. However, based on this discussion, the two experiments described in Sect. 9 and (or variants thereof) could provide a clear test for a time-varying decay parameter.

We conclude the discussion of "flat regions" with a brief mention of possible medical implications. Data taken at Purdue in the period ~2006 November 11–13 indicated a "flat region" during which the measured half-life was $T_{1/2}(^{54}\mathrm{Mn}) \cong 1953$ d, whereas the half-life determined during the preceding month was $\cong 313.5$ d, in reasonable agreement with the published value of 312.12(6) d. Since hints of flat regions also exist in the ^{152}Eu data, this phenomenon may be more general. If flat regions reflect a change in the actual decay rate, as opposed to an instrumental effect which only modifies the count-rate, then one implication is that patients being treated with radionuclides may on occasion be receiving a radiation dose which is significantly different from what has been prescribed. At present it is too early to say whether this would be a concern in practice.

We turn next to a discussion of the phenomenology associated with a periodically varying decay parameter which, as noted previously, may describe effects similar to those seen in the BNL and PTB data. Although it might be naively thought that in such a circumstance the time dependent contributions average out, we will see below that this is not necessarily so.

For the sake of illustration we consider the case

$$\frac{dN(t)}{dt} = -\big(\lambda_0 + 2\Lambda \sin^2(\omega t)\big)N(t) \tag{10}$$

where Λ is a dimensional constant. Solving for $N(t)$ we find

$$N(t) = N_0 \exp\left[-(\lambda_0 + \Lambda)t + \frac{\Lambda}{2\omega}\sin(2\omega t)\right]. \tag{11}$$

We see from (11) that a periodic perturbation in dN/dt results in an additional periodic contribution in $N(t)$, as might be expected. However, since the periodic variations in (10) and (11) are different, it is possible for different experiments based on these equations to find apparently different values of the decay parameter depending on when and how their data are taken. Moreover, this can happen even in the case where two experiments are using the same technique. For example, consider a direct measurement of $N(t)$. One could measure the decay parameter by plotting $\ln[N(t)]$ and finding the slope of the best-fit line. According to (11), the actual data points should be given by

$$\ln[N(t)] = \ln N_0 + \frac{\Lambda}{2\omega}\sin(2\omega t) - (\lambda_0 + \Lambda)t \tag{12}$$

$$\approx \ln N_0 - \lambda_0 t \qquad \text{when } 2\omega t \ll 1, \tag{13}$$

$$\approx \ln N_0 - (\lambda_0 + \Lambda)t \qquad \text{when } (\lambda_0 + \Lambda)t \gg \frac{\Lambda}{2\omega}. \tag{14}$$

Thus, the slope of the best-fit line for an $N(t)$ experiment running for a total time $T \ll 1/(2\omega)$ would give a decay parameter close to λ_0, whereas the same experiment running for a time $T \gg \Lambda/(2\omega(\Lambda+\lambda_0))$ would give a decay parameter closer to $\lambda_0+\Lambda$. If instead we performed during the same time periods an experiment designed to measure dN/dt, we would plot $\ln(-dN/dt)$ and fit the points to a function of the form $\ln\lambda + \ln N_0 - \lambda t$. Again, one could infer the value of the decay parameter by finding the slope of the best-fit line. In this case, according to (10), the data points should be given by

$$\ln\left[-\frac{dN(t)}{dt}\right] = \ln[\lambda_0 + 2\Lambda\sin^2(\omega t)] + \ln N_0 + \frac{\Lambda}{2\omega}\sin(2\omega t) - (\lambda_0+\Lambda)t. \qquad (15)$$

Again we see that the slope of a best-fit line for an experiment of duration $T \ll 1/(2\omega)$ gives a different decay parameter than an experiment of duration $T \gg \Lambda/(2\omega(\Lambda+\lambda_0))$. Furthermore, during sufficiently small time intervals that the first term on the right-hand side of (15) is non-negligible, then the form of (15) differs from that of (12); thus, an experiment designed to measure $N(t)$ could yield a different value for the decay parameter than an experiment designed to measure $dN(t)/dt$, even when both experiments are conducted during the same time interval. This specific example motivates the general conclusion that, in the presence of a time-dependent decay parameter, there are many possibilities for different groups to infer discrepant (yet technically correct) results for the decay parameter λ (and hence for $T_{1/2}$) depending on when and how their data are taken and analyzed.

5 Modifications of Decay Constants in External Fields

The experimental data presented in Sects. 2 and 3, along with the phenomenological analysis in Sect. 4, raise the possibility that nuclear decay rates are being modified by an external source. In the next two sections we consider possible mechanisms which might account for the observed effects. Since the PTB/BNL and flare data are consistent with neutrinos being the source of the time-dependence of $\lambda(t)$, our discussion will focus on neutrinos to illustrate possible mechanisms.

5.1 General Features of Decays in External Fields

We first discuss some of the general features of the process of particle decay in external fields. For external fields that interact only with decay products, i.e. after the decay has happened, one might ask why the external field should have any influence at all on the decay rate. In the case of very strong external fields, a heuristic answer was offered by Reiss (1983), who investigated β-decays in the presence of intense electromagnetic fields. He argued that the field intensity parameter associated with induced beta decay is so large (and the mass of the electron sufficiently small) that the onset of the effective interaction of the electron with the field occurs on a shorter time scale than the Heisenberg uncertainty time ($\Delta t \sim \hbar/(M_W c^2) \sim 10^{-26}$ s) of the beta decay interaction, where M_W is the $W^{\pm}$ boson mass. The onset of the field-electron interaction is also much faster than the transit time of the newly created electron across the nucleus. In such a case, then, one may regard the external field as interacting with the particles *while* they are decaying, and hence the corresponding decay-rate could in principle be modified. If, on the other hand, the decay particles were free of external interaction for some finite (though possibly very small) length of time after the decay occurred, one would not expect the external field to have any appreciable effect on the decay-rate in question.

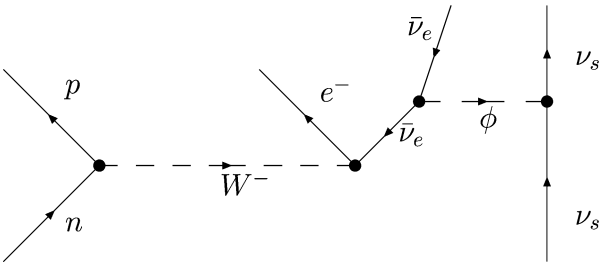

Fig. 11 β-decay modification via a hypothetical short-range scalar interaction between the emitted antineutrino and a single solar neutrino ν_s

By "external field" we will usually mean a non-quantized field which influences a system of interest without back-reaction. Neglecting back-reaction is equivalent to assuming that the interaction with the system causes a negligible phase-space redistribution of the source particles of the external field. This is typically a good approximation if the source of the external field is relatively massive, or is comprised of a very large number of particles. The symmetries of the physical situation dictate how one accounts for energy and momentum conservation in the system interacting with the external field. For example, in the scattering of a system from a static Coulomb potential, the localization of the potential breaks space-translation symmetry, leading to non-conservation of the system's 3-momentum, while the time-independence of the potential guarantees that the system conserves energy. For the case of a system decaying in a time-independent, homogeneous background field, which is discussed in Sect. 5.3, the system's 3-momentum should also be conserved. However, if in this case the external field interacts only with the decay products, one may reasonably regard the system as experiencing a *time-dependent* background, and hence its energy would not be conserved. Note that such arguments are reasonable only if one regards the interaction energy between the system and the background field as belonging solely to the system itself, which is sensible in cases where the external fields experience negligible back-reaction.

We note that if an external field is sufficiently short-ranged, and its source particles sufficiently dilute, a decaying particle is unlikely to interact with more than one source particle of the external field. Unless this one source particle happens to be very massive, it is no longer adequate to ignore back-reaction and treat the external field as described above. In such a circumstance the source particle and its interaction with the decay particles should be explicitly included amongst the other particles and interactions in the S-matrix. As an example, if we consider the hypothetical case of β-decay modified by the interaction of the emitted antineutrino with a sparse sea of solar neutrinos via a short-range scalar interaction, one would presumably need to know the scalar mass and couplings, and then compute the diagram of Fig. 11 as a contribution to the decay-rate. However, given the extreme complexity of the phase-space integrations that arise, it is perhaps prudent to wait to perform this type of calculation until more is known about the specific interaction in question.

5.2 Decays in External Electromagnetic Fields

We next summarize previous work in the literature for the specific case of β-decay in external electromagnetic fields, which serves as a possible model for the more general types of decay-modifications we explore in this paper.

5.2.1 Weak Electromagnetic Fields

In the standard treatment of a weak external electromagnetic field A^{μ}_{ext}, the Lagrangian is modified via the replacement

$$A^{\mu} \rightarrow A^{\mu} + A^{\mu}_{\text{ext}}. \tag{16}$$

Here A^{μ} is quantized in the normal fashion, but A^{μ}_{ext} is regarded as a classical field. One may then carry out perturbative expansions and develop Feynman rules as usual (Bogoliubov and Shirkov 1959; Berestetskii et al. 1979; Mandl and Shaw 1993). This formalism is not adequate when the external field becomes sufficiently strong that its behavior is not accurately described by lower-order perturbative calculations. Given that the modifications to β-decay transition rates are very small even in the presence of very large external electromagnetic fields, this formalism has not commonly been applied to the phenomenon of β-decay, and we shall not discuss it further.

5.2.2 Furry's Formalism for Static Fields; The Phase-Space Prescription

More commonly studied in the literature is the process of β-decay in a very strong external magnetic field. As mentioned above, for strong external fields a prescription of the type (16) is not accurate at lower orders in perturbation theory, and a different formalism is required. One approach was developed by Furry (1951) in an attempt to study quantum electrodynamic processes involving bound states. In this formalism, which is a modified type of interaction picture, the external potential does not explicitly appear in the interaction Hamiltonian, and hence is not quantized, and does not make a direct appearance in any Feynman rules. Rather, the effect of the external field is accounted for by the wavefunctions used in the relevant matrix elements.

An example of Furry's formalism is the calculation of transition rates for β-decay in a constant magnetic field (Matese and O'Connell 1969; Fassio-Canuto 1969; Khalilov 2005). In calculating the decay rate, one would use the standard 4-fermion V-A interaction Hamiltonian

$$\mathcal{H}_{\text{int}} = \frac{G_F}{\sqrt{2}} \int d\mathbf{r} \left[\bar{\psi}_p \gamma_\mu (g_V + g_A \gamma_5) \psi_n\right] \cdot \left[\bar{\psi}_e \gamma^\mu (1 + \gamma_5) \psi_\nu\right], \tag{17}$$

while for the electron wavefunction ψ_e, one would use the solution of the Dirac equation in a constant magnetic field. The relatively small interactions of the external field with the proton and neutron are typically neglected. Referring to the discussion in Sect. 5.1, we assume here that the magnetic field is sufficiently strong that the external electron is never free from the external field. Given that the external field is static, we see that the electron wavefunctions in an external magnetic field serve as the asymptotic states in the calculation. In general, if the time-scale of variations of the external field is much greater than the Heisenberg uncertainty-time of the decay process, it seems reasonable to assume that the decay particle wavefunctions in the presence of the field provide approximate asymptotic states in the calculation. We further note here that since the interaction between the decay system and the magnetic field becomes appreciable only when the electron is produced, it is reasonable to regard the background experienced by the decay system as time-dependent, and hence the system's energy is not conserved. However, the space-translation symmetry of the system's interaction with the background ensures that the system's 3-momentum remains conserved.

The result of the above-described calculation of β-decay in a constant magnetic field yields an important fact, as summarized in Fassio-Canuto (1969): the presence of the magnetic field affects the process only through the electron final-state phase-space volume. The

author further comments that this result is in accordance with the fact that, in the absence of the field, the square of the matrix element, averaged over spins and neutrino directions, does not depend on the electron momentum and neutrino energy. Thus, when the magnetic field is present, no field dependence is exhibited by the matrix element. However, the electron phase-space volume is modified as a result of two influences. It is altered by the presence of the interaction energy of the electron with the magnetic field, $V = -\boldsymbol{\mu}_e \cdot \mathbf{B}$, which may either increase or decrease the energy available to the decay products, depending upon the spin orientation of the emitted electron relative to the field. The phase-space volume is also modified by virtue of quantization of the electron-orbits in the external field, which in general diminishes the number of final states accessible to the electron.

In the case of electromagnetism, the behavior of particles in external fields is well understood. For other types of interactions, it may be difficult or impossible to use Dirac's equation to obtain the wavefunctions needed in Furry's formalism. Furthermore, as mentioned in Sect. 5.1, an exact calculation using Feynman diagrams is also difficult. Thus, rather than directly apply Furry's formalism to decays in general external fields, we seek to apply the prescription described above: that external fields are ultimately accounted for by modifying the phase-space volume available to the decay products. Since we generally do not know what the wavefunction will look like in an external field whose properties are not fully understood, it is difficult (if not impossible) to calculate the phase-space modifications due to energy-level quantization in the external field. As such, we seek to account for the effect of the external field by computing phase-space modifications due solely to the presence of the field's interaction energy with the decay particles. We shall henceforth refer to this as the "phase-space prescription", or the PSP. In Sect. 5.3.2 we investigate the accuracy of the PSP in the specific case of β-decay in external magnetic fields, and find that it predicts decay-rate modifications that are accurate to within an order of magnitude for a wide range of external field strengths.

5.2.3 Extension of Furry's Formalism to Time-Dependent Fields

An extension of this formalism has been developed to deal with time-varying external electromagnetic fields (Nikishov and Ritus 1964; Ritus 1969; Lyul'ka 1975; Ternov et al. 1978; Ternov et al. 1984; Reiss 1983), where again the effect of the external field is solely accounted for by the wavefunctions, which are now time-dependent by virtue of the time-dependence of the electromagnetic background. Reiss (1983) notes that since the external field is time-dependent, the asymptotic states will be time-dependent also, and hence Fermi's Golden Rule cannot be immediately applied. In general, we expect that Fermi's Golden Rule may not apply if variations in the external field cause the asymptotic states to vary on a time-scale which is short compared to the Heisenberg uncertainty time of the decay interaction.

5.3 Decay Modifications by Constant Fields

5.3.1 β-Decay in a Static, Homogeneous, Isotropic Field

By virtue of its computational simplicity, we will first apply the PSP to the case of β-decay in a static field which is isotropic and homogeneous. Practically speaking, such a field would need to be homogeneous and isotropic only over a length scale which is very large compared to the interatomic spacing in a decay sample, and to the de Broglie wavelengths of the decay particles. In such an equipotential region, there is no energy-level quantization, and hence we expect the PSP to be most accurate in this case. We start by considering the decay of a

free neutron at rest. In the absence of an external field, with all form factors approximated as unity, and with the neutrino mass set to zero, the differential transition rate is given by (Griffiths 1987)

$$\frac{d\Gamma}{dE} = \frac{G_F^2}{2\pi^3}\left[\frac{1}{2}(m_n^2 - m_p^2 - m^2)\cdot(E_+^2 - E_-^2) - \frac{2m_n}{3}(E_+^3 - E_-^3)\right], \tag{18}$$

where we have set $\hbar = c = 1$. In (18),

$$E_\pm = \frac{\frac{1}{2}(m_n^2 - m_p^2 + m^2) - m_n E}{m_n - E \mp \sqrt{E^2 - m^2}}, \tag{19}$$

$G_F = 1.166 \times 10^{-5}$ GeV^{-2} is the Fermi constant, m_n, m_p, $m \equiv m_e$ are the neutron, proton, and electron masses, respectively, and E is the energy of the emitted electron. One can simplify this expression by noting that the following quantities are all much smaller than unity:

$$\frac{m_n - m_p}{m_n} \ll 1, \qquad \frac{m}{m_n} \ll 1, \qquad \frac{E}{m_n} \ll 1, \qquad \frac{\sqrt{E^2 - m^2}}{m_n} \ll 1. \tag{20}$$

Expanding (18) in these small parameters and dropping higher-order terms, one obtains

$$\frac{d\Gamma}{dE} \cong \frac{2G_F^2}{\pi^3} E\sqrt{E^2 - m^2}[(m_n - m_p) - E]^2. \tag{21}$$

Note that in this approximation, the parameters m_n and m_p occur only in the combination $m_n - m_p$, and thus rather than regarding $d\Gamma/dE$ as a function of m_n and m_p separately, we may now regard $d\Gamma/dE$ as a function simply of $E_0 \equiv m_n - m_p$, which is the energy available to the decay products:

$$\frac{d\Gamma}{dE} = \frac{2G_F^2}{\pi^3} E\sqrt{E^2 - m^2}(E_0 - E)^2. \tag{22}$$

Before proceeding we note that allowed β-decays are generally similar to free-neutron decay, insofar as these decays are approximately described by (22) with the appropriate E_0. For example, ^{3}H $\rightarrow$ ^{3}He is approximately described by (22), with E_0 set equal to the difference between the ^{3}H and ^{3}He nuclear masses. The fact that the constant prefactor in such decays may differ from $2G_F^2/\pi^3$ is irrelevant in our analysis, since we will be considering fractional changes in transition-rates, in which case the prefactor will divide out. We will thus use (22) to analyze β-decays, with particular emphasis on ^{3}H decay. For forbidden β-decays, the differential transition rate will differ in form from (22) by more than just a prefactor. Thus, for more complicated β-decays such as ^{32}Si$\rightarrow$^{32}P, the analysis presented here is unlikely to be quantitatively applicable, though some of the methods and ideas may be of qualitative value.

We next calculate the effect of the static potential field on the free-neutron decay-rate by applying the PSP to (22). In the presence of an external potential field, the energy balance for the process is given by

$$m_n + V_n = (E_p + V_p) + (E + V_e) + (E_{\bar{\nu}} + V_{\bar{\nu}}), \tag{23}$$

where V_i denotes the interaction energy between particle i and the external field. As we will see in (30) below, and in Fig. 12(a), for almost all values of E_0, energies at least on

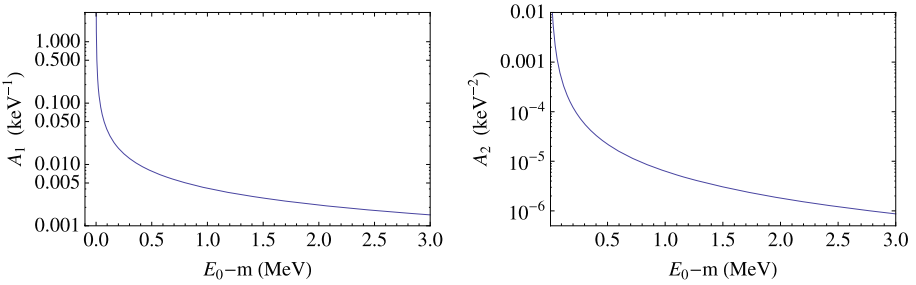

(a) Spin-independent, $|V| \ll E_0 - m$ (b) Spin-dependent, $|V| \ll E_0 - m$

Fig. 12 (**a**) Gives A_1 (in keV^{-1}) versus $E_0 - m$, where A_1 is defined by $\delta\Gamma/\Gamma_0 = A_1 \cdot V$, for $\delta\Gamma/\Gamma_0$ given by (29). (**b**) Gives A_2 (in keV^{-2}) versus $E_0 - m$, where A_2 is defined by $\delta\Gamma/\Gamma_0 = A_2 \cdot V^2$, for $\delta\Gamma/\Gamma_0$ given by (36). In both cases $|V|$ is assumed to be spatially constant

the order of $\gtrsim$1 eV are needed to explain variations on the order of 0.1% (which is the rough scale indicated by the data in Sects. 2 and 3). Since such an energy is substantial on the scale of atomic and low-temperature physics, it may be that the presence of such an external field would be in contradiction with a large body of experiments if it coupled in a spin-independent manner to the proton, neutron, or electron. Although this inference may turn out to be incorrect, we will assume for the present that a static, isotropic, and homogeneous field would couple predominantly to the emitted antineutrino. Setting $V \equiv V_{\bar{\nu}}$ and $V_p = V_e = V_n = 0$, we then have

$$E + E_{\bar{\nu}} = m_n - m_p - V = E_0 - V. \tag{24}$$

It follows that the energy available to the decay products is altered by the presence of the external field such that

$$E_0 \to E_0 - V, \tag{25}$$

and hence the PSP in this case amounts to substituting (25) into (22):

$$\frac{d\Gamma}{dE} = \frac{2G_F^2}{\pi^3} E\sqrt{E^2 - m^2}(E_0 - V - E)^2. \tag{26}$$

We see that, in the case where the interaction affects only the decay products, a negative interaction energy V increases the available phase-space energy, and hence tends to increase the transition rate, while a positive V decreases the available phase-space energy, and tends to decrease the transition rate. Before proceeding, we note that electron-capture transition rates also depend on phase-space factors containing E_0, and the PSP applies straightforwardly in this case.

It is of interest to examine the Kurie function $K(E)$, defined by

$$K(E) \equiv \sqrt{\frac{d\Gamma}{dE} \cdot \frac{1}{E\sqrt{E^2 - m^2}}} = \frac{2G_F^2}{\pi^3}(E_0 - V - E). \tag{27}$$

From (27), we see that when $V \neq 0$, $K(E)$ is obtained by the replacement $E \to E + V$, as noted in Horvat (1998). He further notes that if (27) is modified to include a finite neutrino mass, the Kurie plot is altered in a way that might explain the ^{3}H end-point anomaly, to be

discussed below. Another possible explanation, which we explore in Sect. 5.3.2, is that the neutrino mass is in fact negligible, but that the ^{3}H end-point anomaly may be explained by the presence of a spin-dependent external field.

We now calculate the fractional change in the total transition rate as a result of the external field by integrating equation (26). Using the notation $\tilde{E}_0 = E_0 - V$, we have

$$\Gamma = \int_m^{\tilde{E}_0} dE \frac{d\Gamma}{dE} = \frac{G_F^2}{30\pi^2}\Bigg[\sqrt{\tilde{E}_0^2 - m^2}(2\tilde{E}_0^4 - 9\tilde{E}_0^2 m^2 - 8m^4) + 15\tilde{E}_0 m^4 \ln\left(\frac{\tilde{E}_0 + \sqrt{\tilde{E}_0^2 - m^2}}{m}\right)\Bigg]. \tag{28}$$

Here it is understood that the potential V is always restricted to $V < E_0 - m$, as otherwise the decay is energetically forbidden. There is no energy-balance restriction on negative values of V. We denote the total transition rate in the absence of the field by Γ_0, which is obtained from (28) by setting $\tilde{E}_0 = E_0$. The fractional change in the transition rate in the presence of the field is given by

$$\frac{\delta\Gamma}{\Gamma_0} \equiv \frac{\Gamma - \Gamma_0}{\Gamma_0}. \tag{29}$$

For $|V| \ll E_0 - m$, it can be shown that (29) is approximately linear in V, and hence one may write

$$\delta\Gamma/\Gamma_0 = A_1(E_0) \cdot V, \tag{30}$$

where $A_1(E_0)$ is a function of E_0. A plot of A_1 versus $E_0 - m$ is shown in Fig. 12(a). The results for ^{3}H and free-neutron decay are

$$\left.\frac{\delta\Gamma}{\Gamma_0}\right|_{^3\mathrm{H}} \approx 0.2 \times \left(\frac{V}{1\ \mathrm{keV}}\right), \qquad |V| \ll E_0 - m \approx 18.6\ \mathrm{keV}, \tag{31}$$

$$\left.\frac{\delta\Gamma}{\Gamma_0}\right|_{n} \approx 0.005 \times \left(\frac{V}{1\ \mathrm{keV}}\right), \qquad |V| \ll E_0 - m \approx 780\ \mathrm{keV}. \tag{32}$$

For a given $|V|$, we expect decays with smaller E_0 to experience larger fractional changes in decay-rate. Thus, $V = \pm 200$ eV would give a fractional change on the order of $\pm 0.1\%$ in the transition rate for free-neutron decay, and a fractional change on the order of $\pm 4\%$ in the ^{3}H transition rate. It follows that decay-rates can be very sensitive to small changes in the available phase-space energy. As an example, the matrix elements for free-neutron decay and ^{3}H decay are very similar (neglecting small meson-exchange corrections in ^{3}H), and thus the difference in the respective decay rates is primarily due to the phase-space available to the decay products. Even though E_0 in free-neutron decay is larger than E_0 in ^{3}H decay by only a factor of 2.5, the free-neutron decay rate is larger than the ^{3}H decay rate by a factor of $\approx 6 \times 10^5$. Thus, even potentials that are quite small compared to E_0 are capable of producing observable changes in decay rates.

In the case of a static, spatially constant, isotropic field, the existence of spin-independent potentials V substantially larger than 1 keV is perhaps implausible. However, in Sect. 5.4 we consider the case of time-varying external fields due to solar-neutrinos passing through a sample of radioactive material. In such a circumstance, the interaction energy may become very large for a solar neutrino which passes close to a specific nucleus. Thus, because it will

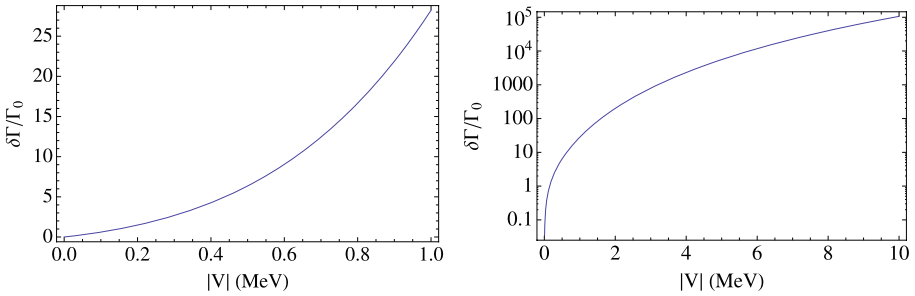

Fig. 13 The fractional change in the free-neutron decay rate, $\delta\Gamma/\Gamma_0$, predicted by the PSP formalism for a static, homogeneous, isotropic, spin-dependent potential field which has an interaction energy $V = -|V|$ with the emitted antineutrino. These plots were generated using (35), which uses the proper relativistic integration limits. Note that the same function is exhibited in both plots, but the vertical scales are linear (*left*) and log (*right*)

have some relevance in Sect. 5.4, the exact fractional change in transition rate as a function of $|V|$ up to 1 GeV is plotted in Fig. 13. Nonetheless, it very well may be that the current formalism breaks down at such large interaction energies.

We note here that for sufficiently large negative values of V, some care is needed with regard to the upper integration limit in (28). The limit $E_{\max} = E_0 - V$ assumes that the parent nucleus is left with negligible kinetic energy. However, since the additional amount of energy $-V$ is available to all the decay products, at sufficiently high negative V, the proton can acquire a significant amount of kinetic energy. The electron attains its maximum energy when its 3-momentum $\mathbf{p}$ is equal and opposite to that of the daughter nucleus, while the neutrino is emitted at rest. For a parent P which β-decays to a daughter D, the energy balance is

$$m_{\mathrm{P}} - V = E_{\mathrm{D}} + E_{\max} = \sqrt{m_{\mathrm{D}} + p^2} + \sqrt{m^2 + p^2}. \tag{33}$$

Solving for $p \equiv |\mathbf{p}|$ gives the maximum electron energy

$$E_{\max}(V) = \sqrt{m^2 + p^2} = \frac{1}{2}\sqrt{\frac{m^2 + (m_{\mathrm{P}} - V)^2 - m_{\mathrm{D}}^2}{m_{\mathrm{P}} - V}}, \tag{34}$$

where again we restrict the potential to $V < m_{\mathrm{P}} - m_{\mathrm{D}} - m$. For free-neutron decay, the maximum electron energy given by (34) is very close to $E_0 - V$ up to $V \sim 25$ MeV, after which point they start to differ significantly. Since different nuclei will have differing points of divergence, it is generally more accurate to use

$$\Gamma = \Gamma(V) = \int_m^{E_{\max}(V)} dE \frac{d\Gamma}{dE} = \int_m^{E_{\max}(V)} dE \frac{2G_F^2}{\pi^3} E\sqrt{E^2 - m^2}(E_0 - V - E)^2, \tag{35}$$

with $E_{\max}(V)$ given by (34), and hence Fig. 13 exhibits plots derived from (35), and not (28).

We now proceed to discuss a point related to the interpretation of the PSP used in (25). In (21) we rightly identify the factor $E_0 \equiv m_n - m_p$ as the energy available to the decay products, assuming zero proton recoil kinetic energy. However, the constants m_n and m_p that appear in (21) arise from factors of m_n and m_p that appear in the invariant amplitude, as well as in the energy-balance-derived integration limits used at earlier stages in the calculation.

Hence, it is not completely clear that in modifying E_0 in (21), one is modifying only the phase-space. Consistent with this concern is the observation that the functional dependence of (18) on m_n and m_p is not simply through the combination $E_0 = m_n - m_p$. It is perhaps more accurate to regard the PSP in this context as describing the decay of a neutron of mass $m_n - V$. Although this makes sense for a neutron at rest, whose entire mass becomes energy available to the decay products, (just as $-V$ is the energy available to the decay products), if the neutron mass is significantly altered, it is not clear that the approximations in (20) continue to hold. Furthermore, it may not make sense to regard the interaction energy V as modifying the masses of the proton, electron, or the antineutrino: not only because one could easily end up with negative masses and various kinematic absurdities, but also because in such a case the energy $-V$ is no longer energy that is available to all the decay products in the same fashion as the neutron rest energy. There is thus some degree of ambiguity in how to accurately account for the presence of V within the PSP formalism. However, these concerns are mitigated by the fact that for potentials $|V| \lesssim 1$ GeV, the fractional variation in transition rate computed using Eqs. (18) and (19), with a neutron mass $m_n - V$, and with the integration limit given by (34), agrees with the fractional variation given by (35) to within an order of magnitude. Thus, while there may be other reasons why the calculation becomes invalid for such large $|V|$, it appears that there is some level of internal consistency in using (35) for $|V| \lesssim 1$ GeV.

5.3.2 β-Decay in a Static, Homogeneous, Spin-Dependent Field

We now consider β-decays in the presence of a static, homogeneous, spin-dependent field, which is of some interest for a number of reasons. First, as discussed in Sect. 5.2.2, it is a case that has been well investigated in the context of β-decay in constant magnetic fields. As such, this allows for a comparison between our PSP formalism and the exact calculations found in the literature. Secondly, for an external field coupling to the proton, neutron, or electron, it may be more likely that the field is spin-dependent, rather than spin-independent, given that the experimental limits on spin-dependent interactions are much less stringent (Fischbach and Talmadge 1999; Fischbach and Krause 1999a, 1999b; Adelberger et al. 2003). Finally, as we will see shortly, such an interaction may offer a novel explanation of the ^{3}H end-point anomaly.

We consider the β-decay of a sample of unpolarized nuclei, and for definiteness we assume that the external field interacts significantly with only one of the decay particles. When comparing our PSP calculation with earlier calculations in the literature for β-decay in magnetic fields, we will assume that this interaction is with the emitted electron. For all other calculations in this section we shall continue to assume that the interaction is with the emitted antineutrino, and in both cases we will denote the interaction energy with the field by V.

In the case of a spin-dependent field we cannot regard all nuclei in the sample as experiencing the same potential. (As we will discuss below, it is precisely this feature of spin-dependent interactions which may explain the ^{3}H end-point anomaly, specifically the fact that determinations of m_ν^2 from the ^{3}H end-point give negative values (Amsler et al. 2008).) For the case of the emitted electron coupling to a magnetic field, the interaction energy $V = -\boldsymbol{\mu}_e \cdot \mathbf{B}$ (where $\boldsymbol{\mu}_e$ is the electron magnetic dipole moment) depends upon the orientation of the magnetic moment $\boldsymbol{\mu}_e$ of the emitted electron relative to $\mathbf{B}$. We note that a sufficiently strong magnetic field can significantly influence the likelihood of the electron being emitted with a certain spin orientation. For a strong enough field, decays in which an electron is emitted with its spin (magnetic moment) in a direction parallel (antiparallel) with the magnetic field are energetically blocked.

While it may be possible to implement the PSP by not performing the angular integrations in the formulae leading to (18) until an angular-dependent V is accounted for in the phase space, we simplify our discussion by adopting the following model. To approximate a sample of unpolarized decaying nuclei, we imagine that half of the decays produce electrons which experience $V = +\mu_e B$, while the other half of the decays produce electrons which experience $V = -\mu_e B$. The average transition rate for a sample of decaying nuclei then becomes

$$\langle \Gamma \rangle \equiv \lambda = \frac{1}{2}\Gamma(-|V|) + \frac{1}{2}\Gamma(+|V|)\Theta(E_0 - m - |V|) \tag{36}$$

where $\Gamma(V)$ is given by (35), and $|V| = |\mu_e B|$. The step-function, $\Theta(x) = 1$ for $x \geq 0$, $\Theta(x) = 0$ for $x < 0$, accounts for the possible energy-blocking of decays with electron spin emitted antiparallel to the magnetic field. Here we introduce the symbol λ to denote the overall, average transition rate for a sample comprised of nuclei which may individually have differing transition rates. A more accurate model would involve an actual averaging over the spin directions of the emitted electrons. Furthermore, it is clear that for sufficiently strong fields, practically all of the decays will experience $V = -|V|$, so that (36) may be in error by a factor of $\sim$2. Given that we are primarily interested in order-of-magnitude estimates for an unpolarized sample, (36) should be adequate for present purposes. We note, however, that the above model could give inaccurate fractional decay-rate variations if there happens to exist a range of $|V|$ where decays with $V = +|V|$ are significantly blocked (so that the above factors of 1/2 become inaccurate), while at the same time $\delta\Gamma(-|V|)/\Gamma_0 \lesssim 1$. For ^{3}H decay, we note that $\delta\Gamma(-|V|)/\Gamma_0 \lesssim 1$ occurs only for $|V| < 500$ eV, which is an energy sufficiently small compared to $E_0 - m \approx 18$ keV that decays with $V = +|V|$ should not be significantly blocked. For an allowed β-decay with $E_0 - m \gtrsim 500$ eV, which includes free-neutron decay, there is no problematic range of $|V|$, although for decays where this is not the case, a more accurate analysis is necessary.

For $|V| \ll E_0 - m$, it can be shown that (29) is approximately quadratic in V, and hence one may write $\delta\Gamma/\Gamma_0 \equiv (\langle\Gamma\rangle - \Gamma_0)/\Gamma_0 = A_2(E_0) \cdot V^2$, where $A_2(E_0)$ is a function of E_0. A plot of A_2 versus $E_0 - m$ is shown in Fig. 12(b). The results for ^{3}H and free-neutron decay are

$$\left.\frac{\delta\Gamma}{\Gamma_0}\right|_{^3\mathrm{H}} \approx 0.013 \times \left(\frac{V}{1\ \mathrm{keV}}\right)^2, \quad |V| \ll E_0 - m = 18.6\ \mathrm{keV}, \tag{37}$$

$$\left.\frac{\delta\Gamma}{\Gamma_0}\right|_{n} \approx 10^{-5} \times \left(\frac{V}{1\ \mathrm{keV}}\right)^2, \quad |V| \ll E_0 - m = 780\ \ \mathrm{keV}. \tag{38}$$

Comparing (37) and (38) with (31) and (32), we see that for a given $|V| \lesssim 1$ keV, the fractional change in decay rate is smaller for the spin-dependent potential. This is expected, given that half of the nuclei decay with $V = +|V|$ and experience a decrease in transition rate which largely cancels the increase in rate experienced by the half of the nuclei which decay with $V = -|V|$. As $|V|$ grows larger, eventually the $V = +|V|$ decays become significantly blocked in the spin-dependent field, and by this point the fractional modifications to decay rates are almost identical for the spin-dependent and the spin-independent fields.

Before proceeding to discuss the modification to the β-decay spectrum, we pause to compare our PSP calculation, applied in the simplified model of (36), to exact calculations performed in the literature for the case of free-neutron decay in strong magnetic fields. We have computed the ratio of the fractional change in decay-rates predicted by our calculation to those of the exact calculation (Matese and O'Connell (1969), (18)). This ratio is less

than 10 for $|V| \lesssim 1$ MeV, corresponding to magnetic fields $B \lesssim 3 \times 10^{14}$ G, although the discrepancy between the two methods grows quite large for stronger magnetic fields. Such a discrepancy is not surprising given that the gap between electron energy levels increases with increasing magnetic field strength, while our calculation ignores phase-space modifications from quantization effects due to the external field. Thus, the PSP formalism may be inapplicable for sufficiently strong static homogeneous spin-dependent fields (or any field where quantization effects become important).

We now discuss the modification to the β-decay spectrum due to the spin-dependent field. To simplify the discussion, we will assume that $|V| \ll E_0 - m$, so that factors of $1/2$ in (36) are fairly accurate. Using (26), the differential transition rate is

$$\left\langle \frac{d\Gamma}{dE} \right\rangle = \frac{1}{2}\frac{d\Gamma}{dE}\bigg|_{V=-|V|} + \frac{1}{2}\frac{d\Gamma}{dE}\bigg|_{V=+|V|}$$
$$= \begin{cases} 2\frac{G_F^2}{\pi^3} E\sqrt{E^2-m^2}((E_0-E)^2+V^2) & \text{for } E \le E_0 - |V|, \\ \frac{G_F^2}{\pi^3} E\sqrt{E^2-m^2}(E_0+|V|-E)^2 & \text{for } E_0 - |V| < E \le E_0 + |V|, \end{cases} \tag{39}$$

where the piecewise structure arises from the fact that the $V = +|V|$ and $V = -|V|$ nuclei have different electron end-point energies. We note that (39) bears an interesting resemblance to the expression for the electron spectrum in the absence of an external field, but where the neutrino mass m_ν is included (Fukugita and Yanagida 2003, p. 263):

$$\frac{d\Gamma}{dE} = \frac{2G_F^2}{\pi^3} E\sqrt{E^2-m^2}\cdot(E_0-E)\sqrt{(E_0-E)^2-m_\nu^2}. \tag{40}$$

For electron energies E sufficiently far from the end-point such that $m_\nu^2 \ll (E_0-E)^2$, we may expand (40) in powers of $m_\nu^2/(E_0-E)^2$ and, dropping higher order terms, we obtain

$$\frac{d\Gamma}{dE} \cong \frac{2G_F^2}{\pi^3} E\sqrt{E^2-m^2}\left((E_0-E)^2 - \frac{1}{2}m_\nu^2\right). \tag{41}$$

Comparing (41) and (39) for $E \le E_0 - |V|$, we see that in the region $V^2 \ll (E_0-E)^2$, *if we set* $V^2 = -m_\nu^2/2$, *then a massless neutrino spectrum in the presence of a spatially constant, spin-dependent real potential* $\pm V$ *is identical to a spectrum with no external field but with negative* m_ν^2. This is quite interesting given that most experiments which fit ^{3}H end-point data to a function of the form (40) obtain a negative best-fit value of m_ν^2 (Amsler et al. 2008). Consider, for example, the experiment of Stoeffl and Decman (1995) who find $m_\nu^2 = -130$ eV^2. From the previous discussion, a possible explanation of their data is the presence of a long-range spin-dependent field which couples to the final-state neutrino with an interaction energy of $|V| \approx \sqrt{65}$ eV. While these two spectra do look different very close to the end-point, where $(E_0-E)^2 \lesssim V^2$, counting statistics are generally poor in this region, and the difference may be difficult to resolve in an experiment. Such a mechanism predicts that the electron spectrum should extend past the expected E_0 by $\sim|V|$, though again it may be difficult to resolve this in practice. Figure 14 shows Kurie plots for ^{3}H for $V^2 = 0$, $V^2 = 65$ eV^2, and $m_\nu^2 = \pm 130$ eV^2. Returning to the discussion at the beginning of this subsection, we see from (36) that what allows an external potential V to simulate a negative value of m_ν^2 is precisely the fact that V is spin-dependent. In the present simplified model of an unpolarized sample, this spin-dependence leads to two distinct populations of decaying nuclei, those whose interactions are $\pm|V|$. It is straightforward to show that for

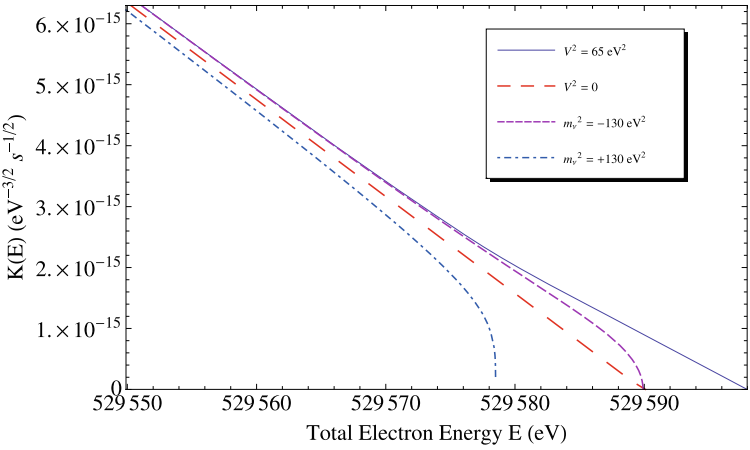

Fig. 14 The Kurie plot for ^{3}H decay, demonstrating how a static, spatially-dependent and spin-dependent potential V produces a Kurie function which mimics the experimentally observed anomalous end-point behavior. The *straight dashed line* is the Kurie function for $V^2 = 0$, $m_\nu^2 = 0$, and intersects the *horizontal axis* at $E = E_0 \approx 529$ keV. The *dotted-dashed curve* which bends down from the straight line is the Kurie function corresponding to (40) for $m_\nu^2 = +130$ eV^2, while the *dashed line* which curves down at E_0 is the Kurie function for (40) with $m_\nu^2 = -130$ eV^2. The *solid line* is the Kurie function for (39) with $V^2 = 65$ eV^2. Note that the *solid line* tracks the $m_\nu^2 = -130$ eV^2 curve quite well except for E within $\sim$10 eV of the end-point, and that outside this region they both curve upward relative to the expected straight-line Kurie function

a spin-independent interaction, where all nuclei would see the same potential V, the Kurie plot would remain a straight line (rather than being curved as in the case $m_\nu^2 \neq 0$), with the only change being $E_0 \to \tilde{E}_0 = E_0 - V$.

It is important to point out that the anomalous ^{3}H end-point behavior does not depend upon a *variation* in the external field, but only on the *presence* of an external spin-dependent field. This is to be contrasted with the data described in Sect. 2, where the oscillatory signal is presumably a manifestation of a $\sim$7% *variation* of the field seen by the nuclear sample. These two situations can provide complementary information on the mechanism in question. In the former case one can roughly infer the absolute scale of the potential interaction in question (within the PSP model described above), while in the latter case one can roughly infer the absolute scale of the fractional change in decay rate due to the presence of the mean external field.

5.4 Decay Modifications from Time-Dependent External Fields

The correlation of the BNL and PTB data with the Earth–Sun distance, combined with the solar-flare data for ^{54}Mn, suggests the possibility that nuclear decay rates are being modified via an interaction with solar neutrinos. As reported in Jenkins and Fischbach (2008), this picture is suggested by the coincidence in time between the occurrence of the solar flare of 2006 December 13, and a dip in the ^{54}Mn count-rate which was detected on the dark side of the Earth. Given that the density of solar neutrinos ν_s at the Earth is $\rho_{\nu_s} \approx 1$ cm^{-3} (Fukugita and Yanagida 2003), an interaction range $\gg 1$ cm would result in a potential field which is sufficiently homogeneous and static that the results of Sect. 5.3 should be applicable. For an interaction range $\ll 1$ cm, the external field experienced by an individual nucleus could vary rather rapidly in time. Hence, we require a more general formalism that is capable of

describing decay processes in an external field with significant time-dependence. We have developed a formalism which partially addresses some of the issues involved, but which does not completely resolve these issues. We nonetheless present the formalism we have developed, in the hope that it offers a starting point for further work which will result in more robust calculational schemes.

As discussed in Sect. 5.2.3, β-decay in a time-varying electromagnetic field has been previously investigated (Nikishov and Ritus 1964; Ritus 1969; Lyul'ka 1975; Ternov et al. 1978; Ternov et al. 1984; Reiss 1983). Such a case allows for an extension of Furry's formalism, as one can solve for the now time-dependent electron wavefunction in the presence of the external electromagnetic field. However, for more general background fields, one typically cannot use the Dirac equation to solve for the wavefunctions, and thus we will again be resorting to the phase-space prescription (PSP).

We note immediately that in the case of the decay particles interacting with a single solar neutrino, one can no longer regard the source of the external field as experiencing negligible back-reaction. Our calculation will nonetheless neglect changes in the solar neutrino phase space, though this could be a large source of error, especially for the case when the interaction energy V is comparable to the solar neutrino single-particle energy. Perhaps a complete computation in this case would involve the evaluation of Feynman diagrams similar to Fig. 11. With this significant caveat in mind, we shall nonetheless proceed with the naive PSP calculation, as it may turn out to give a rough order-of-magnitude estimate of the effect.

We begin by considering the general case of a particle which experiences a time-dependent transition rate $\Gamma(t)$. At this stage the origin of the time variation of Γ is not specified, though we may imagine it arises from a time-dependent potential. From (4), the general solution for the survival probability $P(T)$ is

$$P(T) = \exp\left[-\int_0^T dt\, \Gamma(t)\right], \tag{42}$$

where we have set $P(0) = 1$. For a sample which initially contains N_0 active nuclei, each with a different transition rate $\Gamma_i(t)$ (and hence a different probability of survival $P_i(t)$), the expected number of nuclei remaining at a time T is then

$$N(T) = \sum_{i=1}^{N_0} P_i(T) = \sum_{i=1}^{N_0} \exp\left[-\int_0^T dt\, \Gamma_i(t)\right]. \tag{43}$$

The instantaneous decay rate $dN(T)/dt$ and electron energy spectrum of the sample $d\Gamma(T)/dE$ at time T are then given by

$$\frac{dN(T)}{dT} = -\sum_{i=1}^{N_0} \Gamma_i(T) \exp\left[-\int_0^T dt\, \Gamma_i(t)\right], \tag{44}$$

$$\frac{d\Gamma(T)}{dE} = \sum_{i=1}^{N_0} \frac{d\Gamma_i(T)}{dE} \exp\left[-\int_0^T dt\, \Gamma_i(t)\right]. \tag{45}$$

Depending upon the nature of the time-variation of the individual transition rates, an exact analytical evaluation of these formulae could be quite difficult. Hence, in the general case, a Monte-Carlo computer simulation of the system may be the only way to obtain accurate results. Here we will present a simplified analysis which is valid when (42) is close to unity

for all nuclei in the sample. While this requirement does allow for an analytic calculation, it ultimately seems to yield unobservably small fractional sample decay rate modifications.

We can cast our physical problem into a more manageable form as follows. According to (42), the probability of decay P_D for the nucleus in a time-interval T is given by

$$P_D = 1 - \exp\left[-\int_0^T dt\, \Gamma(t)\right]. \tag{46}$$

Assuming that the nucleus is unlikely to decay during the time T, we have

$$\int_0^T dt\, \Gamma(t) \ll 1, \tag{47}$$

and so to leading order

$$P_D \simeq \int_0^T dt\, \Gamma(t). \tag{48}$$

We now approximate the integral by considering a discrete sum over time intervals $\Delta t = T/n$, where n is sufficiently large that $\Gamma(t)$ is roughly constant over any such time interval Δt. We label these time-intervals by the integer-valued index j, so that the transition rate during the time-interval $t = \Delta t \cdot j \to \Delta t \cdot (j+1)$ is denoted Γ_j. We then have

$$\int_0^T dt\, \Gamma(t) = \sum_{j=0}^{n-1} \Gamma_j \Delta t. \tag{49}$$

Thus, at least as regards the statistically expected number of decays, whenever (47) is satisfied, *observing a single nucleus with transition rate $\Gamma(t)$ for a time T is equivalent to observing for a time $\Delta t = T/n$ an ensemble of n nuclei, each with a generally different time-independent transition rate $\Gamma_j = \Gamma(j \cdot \Delta t)$*. If (47) is not satisfied, the expected number of decays is much larger in the ensemble than for the single nucleus. We may easily extend this picture to a collection of N nuclei, which are labeled by the index i. The expected number of decays during a time T is then

$$\sum_{i=1}^{N} \int_0^T dt\, \Gamma_i(t) = \sum_{i=1}^{N} \sum_{j=0}^{n-1} \Gamma_{ij} \Delta t, \tag{50}$$

where Γ_{ij} is the transition rate for nucleus i during the j^{th} time-interval Δt. The right hand side effectively describes an ensemble of $N \cdot n$ different nuclei which are observed for a time Δt.

We can now define an overall, effective transition rate λ for the sample of N nuclei by

$$N \cdot \lambda \cdot T \equiv \sum_{i=1}^{N} \int_0^T dt\, \Gamma_i(t) = \sum_{i=1}^{N} \sum_{j=0}^{n-1} \Gamma_{ij} \Delta t, \tag{51}$$

so that

$$\lambda = \frac{1}{N \cdot T} \sum_{i=1}^{N} \sum_{j=0}^{n-1} \Delta t\, \Gamma_{ij} = \frac{1}{N \cdot n} \sum_{i=1}^{N} \sum_{j=0}^{n-1} \Gamma_{ij} \equiv \langle \Gamma \rangle, \tag{52}$$

where the right-hand side of (52) is simply the arithmetic ensemble average of Γ_{ij}. Given that we require (47) to hold for all nuclei, $\lambda \cdot T \ll 1$ is automatically satisfied, and hence this formalism demands that $(N(T) - N)/N \ll 1$, where N is the initial number of active nuclei.

For the case of β-decay, we follow (52) in defining the overall, effective differential transition rate $d\lambda/dE$, which gives the observed electron spectrum:

$$\frac{d\lambda}{dE} = \frac{1}{N \cdot n} \sum_{i=1}^{N} \sum_{j=0}^{n-1} \frac{d\Gamma_{ij}}{dE} \equiv \left\langle \frac{d\Gamma}{dE} \right\rangle, \tag{53}$$

where the right-hand side is simply the ensemble average of $d\Gamma_{ij}/dE$ for a given value of the electron-energy E. In doing numerical computations of (53), especially for $E > E_0$, one must either carefully control integration limits or use step-functions, because the analytic formulae for $d\Gamma/dE$ are defined mathematically even for non-physical ranges of E.

Having established some general results, we now consider the specific case of nuclei interacting with solar neutrinos. In the case of a homogeneous, isotropic, and static potential field, the discussion following (23) suggests that the solar neutrinos are likely not interacting with either the neutrons, protons, or electrons, given that the energies involved would probably give rise to effects that contradict existing experiments. For example, for a sufficiently high solar neutrino flux a spin–spin coupling to nucleons or electrons could lead to a polarization of ordinary matter at a level incompatible with observation. However, in the case of a short-range interaction, the *intermittence* of significant potential interactions between a solar neutrino and any of the decay particles may very well give rise to effects that are not detectable in many types of traditional experiments. Thus, it is possible that a short-ranged solar neutrino interaction could allow for a coupling to not only the emitted antineutrino, but also to the nucleons and the electrons. For concreteness, and also for reasons of continuity and comparison with Sect. 5.3, we shall (arbitrarily) assume that the solar neutrinos are interacting with the emitted antineutrino; however, the formalism we present extends in a straightforward way to interactions with the nucleons or electrons. In this regard, we note that in the event of a spin-dependent solar-neutrino coupling to the nucleons, the possibility of preparing a polarized sample of parent nuclei may allow the proposed mechanism to be amplified to a level that would not be attainable for an interaction with the emitted antineutrino (whose unperturbed spin-distribution is isotropic).

We now consider the specific case of nuclei interacting with solar neutrinos via a spin-independent potential, so that V is a function of the nucleus-neutrino separation only. If the interaction potential has a range much shorter than the average distance between two solar neutrinos, each nucleus can be considered to be interacting significantly with at most one neutrino at a given time. As solar neutrinos stream through the nuclear sample, the distance $r(t)$ between a given nucleus i and the closest solar neutrino is changing with time, and hence the interaction potential $V_i(r(t))$ experienced by the nucleus is also changing with time. As a result, according to the phase-space prescription, each nucleus i is characterized by a time-dependent transition rate $\Gamma_i(t) = \Gamma(V_i(r(t)))$. Recalling that the ensemble of (52) is composed of a system of $N \cdot n$ nuclei, observed for a time $\Delta t = T/n$, each with a time-independent Γ_{ij}, we see that different members of the ensemble are distinguished solely by the $V(r)$ which they experience. Thus, one could compute $\langle \Gamma \rangle$ if there were a method for computing the fraction $f(r)dr$ of the ensemble which experiences a potential in the range

$V(r) \to V(r+dr)$:

$$\lambda = \langle \Gamma \rangle = \frac{1}{N \cdot n} \sum_{i=1}^{N} \sum_{j=0}^{n-1} \Gamma_{ij} = \int_0^\infty f(r) dr \cdot \Gamma(V(r)). \tag{54}$$

Similarly, in the case of β-decay, the differential transition rate is given by

$$\frac{d\lambda}{dE} = \left\langle \frac{d\Gamma}{dE} \right\rangle = \int_0^\infty f(r) dr \cdot \frac{d\Gamma(V(r))}{dE} \cdot \Theta(E_0 - E - V(r)), \tag{55}$$

where the step-function $\Theta(x) = 1$ for $x \geq 0$, $\Theta(x) = 0$ for $x < 0$, accounts for the fact that decays with electron energy $E > E_0 - V$ are energetically blocked.

If the potential is spin-dependent, we adopt the simplified model of Sect. 5.3.2. Suppressing the explicit spin-orientation dependence of the potential, and defining $|V(r)|$ to be the maximum positive potential attainable at r, we then have that

$$\lambda = \langle \Gamma \rangle = \int_0^\infty f(r) dr \cdot \frac{1}{2} [\Gamma(+|V(r)|) + \Gamma(-|V(r)|)], \tag{56}$$

and

$$\frac{d\lambda}{dE} = \left\langle \frac{d\Gamma}{dE} \right\rangle = \int_0^\infty f(r) dr \cdot \frac{1}{2} \cdot \left[\frac{d\Gamma(+|V(r)|)}{dE} \cdot \Theta(E_0 - |V(r)| - E) + \frac{d\Gamma(-|V(r)|)}{dE} \cdot \Theta(E_0 + |V(r)| - E) \right]. \tag{57}$$

We further note here that neglecting back-reaction on the solar neutrinos implies that they traverse the sample in a straight line at constant speed.

If the density of solar neutrinos is ρ_ν, then the mean separation between solar neutrinos is $l \sim \rho_\nu^{-1/3}$, and it is unlikely that the closest solar neutrino to a nucleus would be much farther away than l. Thus, in computing (54), one can replace the upper integration limit of ∞ by a distance on the order of l, and approximately calculate $f(r)$ as follows. Consider each of the $N \cdot n$ nuclei in the ensemble described in (52) to be placed at the center of a sphere of volume $1/\rho_\nu$. Each such spherical volume ij is expected to contain roughly one solar neutrino, which is the neutrino closest to the nucleus i during the time step j. If one looks at the larger ensemble, a very large number of different solar neutrinos and nuclei are present, and hence the solar neutrino distribution appears approximately random. Therefore, the fraction of the $N \cdot n$ ensemble nuclei which experience a potential in the range $V(r) \to V(r+dr)$ is given by the probability $P(r)dr$ of finding a neutrino inside a spherical shell of radius r and thickness dr. We thus have

$$f(r)dr = P(r)dr = \frac{\text{volume of shell}}{\text{volume of sphere}} = \frac{4\pi r^2 dr}{1/\rho_\nu} = 4\pi \rho_\nu r^2 dr, \tag{58}$$

and we set the upper integration limit in (54) to be the sphere radius

$$R = \left(\frac{4}{3} \pi \rho_\nu \right)^{-1/3}. \tag{59}$$

Using (54)–(59), we find that for the short-range spin-independent potential, the overall effective transition rate for the sample of N nuclei is given by

$$\lambda = \langle \Gamma \rangle = 4\pi\rho_\nu \int_0^R r^2 \cdot \Gamma(V(r))dr. \tag{60}$$

Hence the overall effective differential transition rate, which yields the electron spectrum, is given by

$$\frac{d\lambda}{dE} = \left\langle \frac{d\Gamma}{dE} \right\rangle = 4\pi\rho_\nu \int_0^R r^2 \cdot \frac{d\Gamma(V(r))}{dE} \cdot \Theta(E_0 - E - V(r)) \cdot dr. \tag{61}$$

For a spin-dependent potential,

$$\lambda = \langle \Gamma \rangle = 4\pi\rho_\nu \int_0^R r^2 \cdot \frac{1}{2} \cdot \big[\Gamma(V(r)) + \Gamma(-V(r))\big]dr, \tag{62}$$

and

$$\frac{d\lambda}{dE} = \left\langle \frac{d\Gamma}{dE} \right\rangle = 4\pi\rho_\nu \int_0^R r^2 \cdot \frac{1}{2} \cdot \left[\frac{d\Gamma(+|V(r)|)}{dE} \cdot \Theta(E_0 - |V(r)| - E) + \frac{d\Gamma(-|V(r)|)}{dE} \cdot \Theta(E_0 + |V(r)| - E) \right] dr. \tag{63}$$

We now demonstrate that the perturbation in a sample's decay parameter is proportional to ρ_ν when the range of the interaction is much smaller than $R \sim \rho_\nu^{-1/3}$. We consider a sample composed of N identical nuclei. Let $\lambda = \lambda_0 + \delta\lambda$, where λ_0 is the decay parameter in the absence of solar neutrinos, and write $\Gamma(V(r)) = \Gamma_0 + \delta\Gamma(V(r))$, where $\Gamma_0 = \lambda_0$ is the transition rate for a single nucleus in the absence of solar neutrinos. Considering the spin-independent potential for simplicity, (60) becomes

$$\lambda_0 + \delta\lambda = 4\pi\rho_\nu \int_0^R r^2 \cdot \big[\Gamma_0 + \delta\Gamma(V(r))\big]dr. \tag{64}$$

By virtue of (59) we then have

$$4\pi\rho_\nu \int_0^R \Gamma_0 r^2 dr = \Gamma_0 = \lambda_0, \tag{65}$$

so that (64) becomes

$$\delta\lambda = 4\pi\rho_\nu \int_0^R r^2 \cdot \delta\Gamma(V(r))dr. \tag{66}$$

Other than the factor of $4\pi\rho_\nu$ multiplying the integral, the only ρ_ν dependence of (66) is through the upper integration limit R. However, if the range (denoted r_0) of the potential V is much less than $R \sim \rho_\nu^{-1/3}$, then we expect that the integrand in (66) is negligible near the upper integration limit R, and in fact is only significant for $r \lesssim r_0$. Hence, the only ρ_ν dependence of (66) is through the factor $4\pi\rho_\nu$, so that $\delta\lambda \propto \rho_\nu$.

5.4.1 Modeling The Interaction Potential

Before presenting numerical results, we first discuss how we are modeling the interaction potential $V(r)$. It is well known that in the center-of-mass frame, the non-relativistic 2-body interaction potential is given by the Fourier-transform of the invariant amplitude computed using Feynman rules. We shall assume that such a prescription holds true for the case of relativistic solar neutrinos interacting with nucleons in the lab frame. There is some precedent for this type of treatment: the MSW effect, describing solar neutrino oscillations in matter, can be treated in a non-relativistic potential picture, as was originally done (Bethe 1986); these results were later confirmed using the full machinery of relativistic quantum field theory (Nieves 1989).

One possible choice of potential would be the pseudoscalar exchange potential (Frauenfelder and Henley 1974):

$$V_{12} = \frac{A}{r^3} \cdot [3(\boldsymbol{\sigma}_1 \cdot \hat{\mathbf{r}})(\boldsymbol{\sigma}_2 \cdot \hat{\mathbf{r}}) - \boldsymbol{\sigma}_1 \cdot \boldsymbol{\sigma}_2], \tag{67}$$

where A is a constant depending upon the pseudoscalar mass and its couplings to the two particles, $\mathbf{r}$ is the separation vector between the particles, and $\boldsymbol{\sigma}_1, \boldsymbol{\sigma}_2$ are the spin orientations of the two particles. When considering spin-dependent interactions between solar neutrinos and nuclear decay products, we have chosen to adopt a simplified model in which the spin-orientation dependence of the potential is suppressed, and the nuclei in the sample are considered to be experiencing a potential

$$V(r) = \pm \frac{B}{r^3}, \tag{68}$$

where B is a spin-independent constant roughly equal to A, and r is the separation between the particles. In such a picture half of the nuclei experience a potential $V = +|V|$ and half experience a potential $V = -|V|$. We note that while the semi-classical potential (68) formally diverges as $r \to 0$, one should not use such a formula for r smaller than the distance at which higher-order corrections start to dramatically modify the interaction in question. This distance is likely to be much smaller than any distance scales in our problem, and specifically this distance is not related to the quantity $r_{\min}$ to be discussed shortly.

As discussed in Sect. 5.3.2, the PSP formalism breaks down at sufficiently high energies. Energy-level quantization and the solar neutrino phase space are also more important at higher energies, and hence it is likely incorrect to use the potential (68) for arbitrarily small values of r. For the interaction of a solar neutrino with an electron, it would be reasonable to suppose that the functional form of $V(r)$ in (68) could remain valid down to distances as small as $\sim 10^{-16}$ cm $\approx 1/M_W$, assuming the semi-classical picture still holds at this energy scale, since existing data support the view that an electron behaves "point-like" down to this scale (Odom et al. 2006). However, since $|V(r)|$ would be sufficiently large at such small distances to violate the approximations we have made in calculating its effects, we will cut off the potential at some value of r, hereafter called $r_{\min}$, defining the potential to be

$$V(r) = \pm \begin{cases} V_{\max} & \text{for } r \le r_{\min}, \\ V_{\max} \cdot (\frac{r_{\min}}{r})^3 & \text{for } r \ge r_{\min}. \end{cases} \tag{69}$$

We stress here that $r_{\min}$ has no physical significance, as it represents only the likely breakdown of our calculational formalism, and hence has no relationship to the range of the potential. Unfortunately, any "leverage" to be gained by the r-dependence of the potential

is thus lost by using (69), which is essentially a step-function as regards order-of-magnitude calculations. Regrettably, then, the specific r-dependence of the potential does not significantly affect the results of our calculation. It follows from the preceding discussion that the numerical results to be presented below, which suggest that the solar neutrinos produce too small an effect to explain existing data, are only valid within the framework of the present approximations. It is thus possible that a more general formalism capable of dealing with smaller values of r, and hence with larger $|V(r)|$ could in fact account for existing data in terms of a spin-dependent $V(r)$.

In any numerical calculation, both $V_{\max}$ and $r_{\min}$ must be set. As mentioned in our previous discussion, in order for the PSP to give accurate values of Γ we are restricted on the range of $V_{\max}$ we may use. We thus choose $V_{\max} = 1$ MeV, which is the rough energy scale of solar neutrinos, noting that the error in neglecting the solar neutrino phase-space redistribution is likely increasingly significant after this point. We also note that this is the energy past which the PSP calculation starts to differ significantly from the exact calculation of Matese and O'Connell (1969), though perhaps this has no bearing on more general interactions. With $V_{\max}$ set, $r_{\min}$ is then essentially a free parameter. We also give results for $V_{\max} = 400$ MeV, where the PSP prescription is still internally consistent, as discussed in Sect. 5.3.1. We regard these results very cautiously, however, given that at these energies the issue of the solar neutrino phase space may become significant and, additionally, the PSP prescription diverges significantly from the results of Matese and O'Connell (1969) in the case of a constant external magnetic field. We note in passing that even for $V_{\max} = 400$ MeV we satisfy the condition in (47) which allows us to generate the ensemble discussed in Sect. 5.4.

We note that, with energies significantly higher than E_0, the use of spin-independent rather than spin-dependent potentials does not result in large changes to the predicted modification of the decay rate. This is in contrast to what was shown in Sect. 5.3.2 where the predicted modification to the decay rates of free neutrons and ^{3}H were significantly smaller for a spin-dependent potential when $|V| \ll E_0$. When $|V| \ll E_0$, the $+|V|$ and $-|V|$ contributions largely cancel, assuming that half of the emitted particles experience $+|V|$ and the other half experience $-|V|$. When $|V| \gg E_0$, a spin-dependent potential energetically forbids decays experiencing $+|V|$, so all decays will experience the $-|V|$ interaction, which is the same as if the potential were spin-independent. Thus, spin-independent potentials essentially give the same results as spin-dependent potentials in the PSP when $|V| \gg E_0$.

The preceding considerations allow us to address the implications of the present formalism for solar dynamics. Given the fact that the density of solar neutrinos in the Sun is far greater than it is on Earth, could the mechanism presented here lead to an unacceptably large decay rate for nuclei undergoing radioactive decay in the Sun? (A similar question arises regarding nucleosynthesis in the early universe.) One possibility is that in the case of a spin–spin interaction the isotropy of the solar neutrinos in the Sun might sum to a largely null interaction energy. Note that this would assume that the spin–spin interaction range is much larger than the mean inter-neutrino spacing, so that the interactions of solar neutrinos could be described by a coherent field rather than as the "ballistic" interaction of individual neutrinos. It may also be the case that the neutrino–nucleus interaction energy is a sufficiently small contribution to the ambient energy density in the Sun, that its presence would not materially affect nuclear decay rates in the Sun. Finally, increasing the neutrino density or flux does not necessarily lead to a monotonic increase in nuclear decay rates, as might naively be thought: increasing λ eventually leads to a more rapid depletion of the population of atoms available to decay, and this is the principle that underlies the SID effect which we discuss in Sect. 9 below. Taken together, these observations suggest that the role of neutrinos in influencing decay rates of nuclei in the Sun requires a more careful analysis.

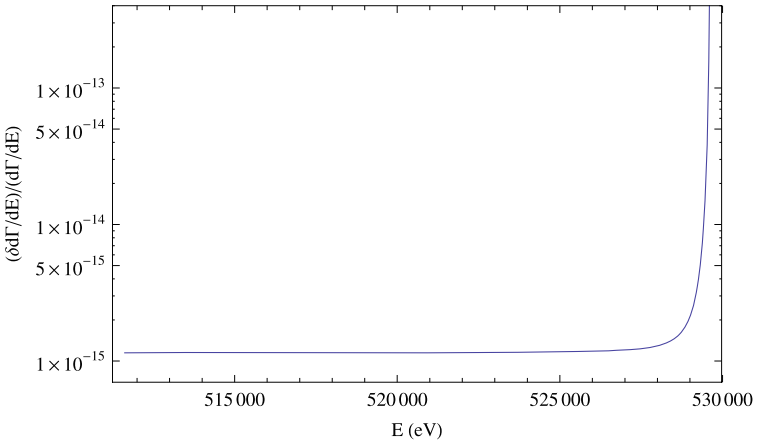

Fig. 15 The fractional change in the spectrum for ^{3}H β-decay for $V_{\max} = 1$ MeV and $r_{\min} = 4.5$ Å. Note that near E_0 where the spectrum is the smallest, the fractional change is the largest. This is expected given that we are now allowing more electrons to decay with energies in that region (and higher)

5.5 Calculational Results

For a spin-dependent potential with $V_{\max} = 1$ MeV, we find that for ^{3}H

$$\frac{\delta\lambda}{\lambda_0} = \frac{\langle\Gamma\rangle - \Gamma_0}{\Gamma_0} = \frac{\delta\Gamma}{\Gamma_0}\bigg|_{^3\mathrm{H}} \approx 1.9 \cdot 10^{-17} \cdot \left(\frac{r_{\min}}{1\ \text{Å}}\right)^3, \tag{70}$$

where $r_{\min} \ll 1$ cm. We study ^{3}H since this is the simplest superallowed decay for which the PSP formalism is applicable. The fractional changes in $\Gamma(^3\mathrm{H})$ are exceedingly small, roughly 12 orders of magnitude smaller than the observed changes in the count-rate in the BNL/PTB data for the nuclides studied by these groups (see Sect. 2). That $\delta\Gamma/\Gamma$ is proportional to $r_{\min}^3$ is expected based on (68). This is because, as mentioned in Sect. 5.4.1, our potential approximates a step-function, and thus $\delta\Gamma/\Gamma$ is proportional to the number of affected nuclei, which is proportional to $r_{\min}^3$. We note that to get a value consistent with the $\sim 0.1\%$ scale characteristic of the BNL/PTB data with $V_{\max} = 1$ MeV, $r_{\min}$ must be increased to $\sim 10^{-6}$ m. This would imply extremely large values of the potential even at relatively large distances (Angstroms), and as such may be an indication that the chosen potential is unphysical. We again emphasize that the large disparity between our calculated results for $\Gamma(^3\mathrm{H})$ and the general order-of-magnitude effects suggested by the BNL/PTB data may simply reflect the limitations of our formalism in dealing with small values of r, where $|V(r)|$ could be large enough to account for the data. It is also possible that the PSP formalism combined with the semi-classical potential picture developed here may not be appropriate. In either case, it is our calculational scheme which is inadequate, and solar neutrino interactions may still be the responsible mechanism.

It is instructive to investigate the electron spectrum to determine the energy range in which the majority of the additional decays are occurring. Figure 15 shows the fractional change in the ^{3}H spectrum for $V_{\max} = 1$ MeV, $r_{\min} = 4.5$ Å. For these values, $\delta\Gamma/\Gamma = 1.7 \times 10^{-15}$. In Fig. 15, we see that for electron energies $m < E < \sim E_0$, the fractional change is one part in 10^{15}, so that the extra decays are spread somewhat evenly throughout the traditional range of electron energies. We also see that near E_0 the fractional change in

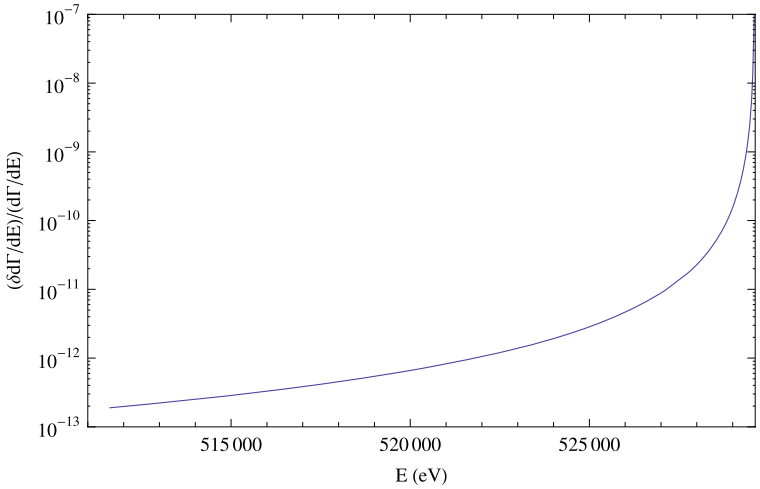

Fig. 16 The fractional change in the spectrum for ^{3}H β-decay for $V_{\max} = 400$ MeV and $r_{\min} = 4.5$ Å. Note that near E_0 where the spectrum is the smallest, the fractional change is the largest. This is expected given that we are now allowing more electrons to decay with energies in that region (and higher)

the spectrum increases by several orders of magnitude. This is expected, as in the absence of an external potential the number of electrons that are emitted with energies near E_0 is relatively small, but in the presence of such a potential there may be many electrons emitted with those energies. There is also a portion of the spectrum that extends beyond E_0, as expected in the presence of the additional energy $|V|$ available to the decay products. For the chosen values of $r_{\min}$ and $V_{\max}$, the fraction of electrons emitted with energies greater than E_0 is $\sim 10^{-15}$, which is on the order of $\delta\Gamma/\Gamma$. We also note that fractional changes on the order of 10^{-15} to 10^{-13} are far too small to explain the ^{3}H end-point, within the present formalism.

In the absence of any restrictions on the range of $V_{\max}$ in the PSP formalism, one can ask what value would be needed to obtain an observable change in the decay rate on the order of 0.1%. Keeping $r_{\min}$ at 4.5 Å, $V_{\max}$ must be increased to ~400 MeV in order to obtain $\delta\Gamma/\Gamma \sim 0.1\%$. A plot of the fractional change in the spectrum for $V_{\max} = 400$ MeV is given in Fig. 16. While the fractional change over energies $m < E < E_0$ is certainly greater than for the 1 MeV case shown in Fig. 15, the greatest contribution to the change in the decay rate comes from electrons with energies greater than E_0, as these make up ~0.1% of the electrons emitted. This would not necessarily be easily seen in the spectrum, however, since the peak beyond E_0 is roughly 7 orders of magnitude smaller than the peak in the range from m to E_0. If this calculation were to accurately model the physical mechanism responsible, the change in the decay rate might not even be detectable in some experiments. For example, an experiment that directly counted β-particles may have discriminators set up to screen out energies greater than E_0, in which case most of the extra signal would be lost. Assuming that the presence of the potential does not significantly alter the state of the daughter products, however, an experiment set up to detect the de-excitation of a daughter state at a fixed energy would be able to detect the modification to the decay rate. We also note that even with $V_{\max}$ at 400 MeV, the modifications to the spectrum near E_0 are far too small to explain the ^{3}H end-point anomaly, within our present calculational framework.

In summary, using values of $r_{\min}$ and $V_{\max}$ most compatible with the PSP formalism as applied to a short-ranged intermittent potential generated by an interaction with solar neutrinos, the resulting changes in decay rates are too small to explain either the PTB/BNL data or the ^{3}H end-point anomaly. While increasing $r_{\min}$ and $V_{\max}$ can give changes in decay rates on the order of the PTB/BNL data, we do not currently know how to justify the required values in the context of the PSP formalism. However, our results certainly do not disprove the hypothesis that solar neutrinos could be influencing decay rates. Leaving aside the fact that ^{3}H was not one of the isotopes used in the BNL/PTB experiments (and may be affected very differently than those used), and that the PSP formalism may break down in the general case, in order to overcome calculational difficulties and limitations some potentially severe additional approximations and assumptions were made. The first was that the scattering of the solar neutrino was negligible, which is almost certainly not true for interaction energies as high as 1 MeV. Thus correctly including the effects of the solar neutrino phase space may give more promising results. The other significant approximation was the implementation of $V_{\max}$, which neglects the increasing strength of the potential at short distances. A calculation which properly addresses these issues would help in understanding the modification of decay rates by solar neutrinos, and thus the possibility that such a mechanism could account for the observed decay data. We finally note that if the solar neutrino interaction in question has a range of $\gg 1$ cm, then the formalism and mechanism of Sect. 5.3 appear to provide for a viable explanation of the observed decay data.

6 Seasonal Variation of the Fine Structure Constant and α-Decay

In this section we discuss a different model which characterizes a class of theories that could lead to a seasonal variation of radioactive decay rates. All decay processes depend on fundamental constants, including the strengths of the electromagnetic, weak, and strong interactions. Recently, several authors have discussed the possibility that the electromagnetic fine structure constant $\alpha_{\rm EM}$ might exhibit a seasonal time dependence (Flambaum and Shuryak 2008; Shaw 2007; Barrow and Shaw 2008). Since both α- and β-decay processes depend on $\alpha_{\rm EM}$ (Uzan 2003), any time variation in $\alpha_{\rm EM}$ could lead to a modulation of the these decay rates.

A seasonal variation in the fine structure constant would occur if the magnitude of $\alpha_{\rm EM}$ depended on a scalar field ϕ produced by the Sun. Since a light scalar field would look like gravity, one can write the relative variation in $\alpha_{\rm EM}$ due to ϕ as Flambaum and Shuryak (2008)

$$\frac{\delta\alpha_{\rm EM}}{\alpha_{\rm EM}} = \frac{k_\alpha \delta U_g}{c^2}, \tag{71}$$

where k_α is a dimensionless parameter, c is the speed of light, and U_g is the gravitational potential. (In this section, we reinstate factors of c.)

For an experiment conducted on the Earth, the greatest variation in the gravitational potential is due to the Earth's motion around the Sun (Flambaum and Shuryak 2008). The eccentricity of the Earth's orbit is small ($\epsilon \simeq 0.0167$), so the Earth–Sun separation can be written as

$$r(t) = r_\oplus + \epsilon r_\oplus \cos\left[\frac{2\pi(t-t_0)}{T}\right] + \mathcal{O}(\epsilon^2), \tag{72}$$

where $r_\oplus$ is the mean Earth–Sun separation, $T = 1$ y is the orbital period, and $t = t_0$ when the Earth is at its aphelion. The Sun's gravitational potential experienced by the Earth is then

$$U_g(r) = -\frac{GM_\odot}{r} \cong -\frac{GM_\odot}{r_\oplus}\left\{1 - \epsilon\cos\left[\frac{2\pi(t-t_0)}{T}\right] + \mathcal{O}(\epsilon^2)\right\}, \tag{73}$$

where $M_\odot$ is the mass of the Sun. Substituting (73) into (71) leads to an expression for the expected seasonal variation in $\alpha_{\rm EM}$:

$$\alpha_{EM}(t) \simeq \alpha_{EM}^\infty + \alpha_{EM}^\infty \frac{k_\alpha \epsilon GM_\odot}{r_\oplus c^2}\cos\left[\frac{2\pi(t-t_0)}{T}\right], \tag{74}$$

where $\alpha_{EM}^\infty \simeq 1/137$ is the value of the fine structure constant when $\phi = 0$, which occurs at $r \to \infty$.

These variations in $\alpha_{\rm EM}$ will affect the α-decay rate of unstable nuclei since the α-particles must tunnel through the Coulomb barrier (for a review, see Uzan 2003). For a nucleus with atomic number Z, one can write its α-decay rate as (Uzan 2003; Hodgson et al. 1997)

$$\Gamma \simeq \Gamma_0(\alpha_{\rm EM}, v)\exp\left[-4\pi Z\alpha_{\rm EM}\frac{c}{v}\right], \tag{75}$$

where $v/c = \sqrt{2Q/m_\alpha c^2}$ is the speed of the emitted α-particle, and m_α is the mass of the α-particle. Q is the total change in the system's binding energy,

$$Q = B(Z-2, A-4) + B(Z=2, A=4) - B(Z, A), \tag{76}$$

where Z (A) is the atomic (mass) number of the nucleus, and $B(Z, A)$ is the associated binding energy. The factor $\Gamma_0(\alpha_{\rm EM}, v)$ has a slow dependence on $\alpha_{\rm EM}$ and v compared to the exponential term and so will be treated as constant.

To determine the effect of the scalar field ϕ on the α-decay rate, we substitute (74) into (75), which gives

$$\begin{aligned}\Gamma(t) &\simeq \tilde{\Gamma}_0\exp\left\{-\alpha_{EM}^\infty\frac{4\pi k_\alpha\epsilon(c/v)ZGM_\odot}{r_\oplus c^2}\cos\left[\frac{2\pi(t-t_0)}{T}\right]\right\},\\ &\simeq \tilde{\Gamma}_0 - \tilde{\Gamma}_0\left\{\alpha_{EM}^\infty\frac{4\pi k_\alpha\epsilon(c/v)ZGM_\odot}{r_\oplus c^2}\cos\left[\frac{2\pi(t-t_0)}{T}\right]\right\},\end{aligned} \tag{77}$$

where

$$\tilde{\Gamma}_0 \equiv \Gamma_0(\alpha_{\rm EM}, v)\exp\left[-4\pi Z\alpha_{\rm EM}^\infty\frac{c}{v}\right], \tag{78}$$

is independent of time. The relative change in the decay rate is then

$$\frac{\delta\Gamma(t)}{\Gamma} \equiv \frac{\Gamma(t)-\tilde{\Gamma}_0}{\tilde{\Gamma}_0} = \left(\frac{\delta\Gamma_0}{\Gamma}\right)_{k_\alpha}\cos\left[\frac{2\pi(t-t_0)}{T}\right], \tag{79}$$

where the amplitude of the relative decay oscillation is

$$\left(\frac{\delta\Gamma_0}{\Gamma}\right)_{k_\alpha} \equiv -\alpha_{EM}^\infty\frac{4\pi k_\alpha\epsilon(c/v)ZGM_\odot}{r_\oplus c^2}. \tag{80}$$

Thus, the effect of ϕ on alpha decay would be a sinusoidal variation in the decay rate in phase (or exactly out of phase, depending on the sign of k_α) with the Earth–Sun separation.

To explain the seasonal variation of the α-decay rate of ^{226}Ra observed recently by the PTB (Siegert et al. 1998), which has an amplitude (Jenkins et al. 2008)

$$\left(\frac{\delta\Gamma_0}{\Gamma}\right)_{\mathrm{Ra}} \sim 3\times 10^{-3}, \tag{81}$$

(80) requires that

$$k_\alpha = \frac{r_\oplus c^2}{4\pi\alpha^\infty_{EM}\epsilon(c/v)ZGM_\odot}\left(\frac{\delta\Gamma_0}{\Gamma}\right)_{\mathrm{Ra}}. \tag{82}$$

Using $Q = 4.9$ MeV for the α-decay of ^{226}Ra (NNDC 2008), $v/c \simeq 0.051$, together with $GM_\odot/r_\oplus c^2 \simeq 9.8\times 10^{-9}$, (82) then gives

$$k_\alpha \simeq 4.5\times 10^7, \tag{83}$$

which is significantly larger than the limit $k_\alpha = (-5.4\pm 5.1)\times 10^{-8}$ obtained by Barrow and Shaw from a recent atomic physics experiment (Rosenband et al. 2008). Therefore it is highly unlikely that the seasonal variation of the ^{226}Ra decay rate seen by the PTB group can be attributed to effects of a single scalar field ϕ. However, this model illustrates how a seasonal variation of a fundamental constant (e.g. α_{EM} or m_e/m_p) affects nuclear decay rates, and it is conceivable that a more elaborate model taking into account variations in more than one fundamental constant could lead to observable effects that would have escaped detection in other experiments.

7 Discussion of Critical Papers

The appearance of our original papers (Jenkins et al. 2008; Jenkins and Fischbach 2008) motivated a search for archived data sets which might contain useful results. Norman et al. (2009) examined data for ^{22}Na, ^{44}Ti, ^{108}Ag$^{\mathrm{m}}$, ^{121}Sn$^{\mathrm{m}}$, ^{133}Ba, and ^{241}Am and found no evidence for an annual variation of these decay rates at a level below that detected in both the BNL and PTB data sets. It is possible that the BNL/PTB data experienced some overlooked (but not fundamental) systematic effect which was not present in the data of Norman et al. (2009). However, since it is likely that different nuclides would be sensitive in different degrees to any external influence, it is also possible that ^{32}Si, ^{36}Cl, and ^{226}Ra are simply more sensitive "detectors" than the nuclides studied by Norman et al. (2009). In any case, although the data in Norman et al. (2009) are quite interesting, they do not necessarily contradict the BNL/PTB data presented in Jenkins et al. (2008), or the solar flare data of Jenkins and Fischbach (2008).

We turn next to the analysis by Cooper (2009) of data from the radioisotope thermoelectric generators (RTGs) obtained from the Cassini mission, searching for a variation of the decay rate of ^{238}Pu as a function of the distance of Cassini from the Sun. The premise of this analysis is that since the energy produced by the RTG comes from ^{238}Pu α-decay, the indication that the PTB data from ^{226}Ra (which is also an α-emitter) shows a variation with the Earth–Sun distance suggests that the Cassini data should as well. Cooper analyzed two years of Cassini data and set a limit of 0.84×10^{-4} on a contribution varying as $1/R^2$ in the ^{238}Pu decay rate. In what follows we temporarily set aside questions about the reliability and interpretations of the RTG data, and assume that Cooper's analysis is correct.

Notwithstanding the fact that ^{238}Pu decays via α-emission, as does ^{226}Ra, there is a difference in their respective decay chains which may play a role in understanding the RTG data. ^{238}Pu ($T_{1/2} = 87.7$ y) decays to ^{234}U ($T_{1/2} = 246{,}000$ y), and hence for practical purposes only α-decays contribute significantly to the Cassini RTG. By way of contrast, the dominant decay chain for ^{226}Ra is more complicated (Chisté et al. 2008): $^{226}\mathrm{Ra} \xrightarrow{1600\,\mathrm{y}} {}^{222}\mathrm{Rn} \xrightarrow{3.8\,\mathrm{d}} {}^{218}\mathrm{Po} \xrightarrow{3.1\,\mathrm{m}} {}^{214}\mathrm{Pb} \xrightarrow{27\,\mathrm{m}} {}^{214}\mathrm{Bi} \xrightarrow{20\,\mathrm{m}} {}^{214}\mathrm{Po} \xrightarrow{160\,\mu\mathrm{s}} {}^{210}\mathrm{Pb} \xrightarrow{22\,\mathrm{y}} {}^{210}\mathrm{Bi} \xrightarrow{5\,\mathrm{d}} {}^{210}\mathrm{Po} \xrightarrow{140\,\mathrm{d}} {}^{206}\mathrm{Pb}$. Thus a sample of ^{226}Ra quickly comes to equilibrium with daughters ^{214}Pb and ^{214}Bi undergoing β-decay (Christmas et al. 1983; Siegert et al. 1998). As noted in Sect. 2, it then follows that if we accept the Cooper analysis at face value, a possible explanation of the ^{226}Ra data (which evidence a time-varying signal), and the Cassini RTG data (which do not) is that the dominant effects of the underlying mechanism appear in β-decays.

Support for this conjecture comes from data reported by Ellis (1990) who used a ^{238}PuBe neutron irradiator to carry out *in vivo* neutron activation analysis in humans. Ellis observed that when the ^{238}PuBe irradiator was used to initiate the reaction $^{55}\mathrm{Mn}(n,\gamma)^{56}\mathrm{Mn}$, the resulting γ counts in the 847 keV photopeak exhibited a "... seasonal difference of approximately 0.5% ... between the winter and summer months." Given that the higher counts occurred during the winter months, Ellis' data agree in both magnitude and phase with the BNL and PTB data. Since both the Cooper and Ellis data depend on ^{238}Pu decay, it is not clear at present what the origin is of the (apparent) discrepancy in the reported data, but one possibility may be problems with modeling the behavior of RTGs in a space environment, or some unknown systematic effect in the Ellis experiment.

8 Discussion of ^{14}C Decay

Following the appearance of Jenkins and Fischbach (2008) and Jenkins et al. (2008), a paper appeared (Sanders 2008) discussing the possible relevance of our work to ^{14}C dating. Here we add a few comments on ^{14}C dating.

Chiu et al. (2007) analyzed data on ^{14}C atmospheric concentrations (denoted by Δ^{14}C) in an effort to understand the causes of Δ^{14}C fluctuations. Although a precise knowledge of $T_{1/2}(^{14}\mathrm{C})$ is not necessary for some dating applications, if ^{14}C dates are calibrated against tree-ring dates, $T_{1/2}(^{14}\mathrm{C})$ is needed to understand and interpret the causes of Δ^{14}C fluctuations. Chiu et al. (2007) give an extensive discussion of the different determinations of $T_{1/2}(^{14}\mathrm{C})$ that have been reported in the literature, along with various discrepancies among the published values.

Returning to the discussions of Sect. 4 and Sect. 5.3, we note that if λ is in fact modified by external fields, some of the reported discrepancies could have arisen from measurements carried out at different times (when the external field had different values), or perhaps through the use of different measurement techniques (see Sect. 4). As an example of the latter effect, consider a comparison of $T_{1/2}(^{14}\mathrm{C})$ obtained from a calorimeter experiment versus a determination of $T_{1/2}(^{14}\mathrm{C})$ by a direct counting experiment conducted at the same time. In the presence of a constant potential interaction V of the type described in Sect. 5.3, the decay parameter λ will differ from its unperturbed value λ_0. The exact modified decay parameter would presumably be measured in a direct counting experiment, and is given by

$$\lambda = \lambda_{\mathrm{count}} = \lambda_0 \cdot \left[1 + \frac{1}{\lambda_0}\int_m^{E_0+|V|} \delta\left(\frac{d\lambda}{dE}\right)\cdot dE\right], \tag{84}$$

where $\delta(d\lambda/dE)$ is the modification to the spectrum due to the potential interaction. However, as we now demonstrate, the calorimetric method may not yield the exact modified

decay parameter. If one knows the number of active nuclei N in the calorimeter, the decay parameter $\lambda_{\rm cal}$ is determined by measuring the collected power P and setting

$$P = N \cdot \overline{K} \cdot \lambda_{\rm cal}, \tag{85}$$

where $\overline{K}$ is the expected mean electron kinetic energy $K = E - m$. *It follows that one can obtain incorrect values of* $\lambda_{\rm cal}$ *if an incorrect value of* $\overline{K}$ *is used.* This may occur if the assumed value of $\overline{K}$ was measured at a time when the external field differed, or if it is computed under the assumption that there is no perturbing external field. For example, in the absence of a perturbing field, $\overline{K}$ for an allowed β-decay with endpoint energy E_0 is given by

$$\overline{K}_0 \equiv \overline{K}|_{V=0} = \frac{1}{\lambda_0}\int_m^{E_0} dE \frac{d\lambda_0}{dE} \cdot K = \frac{\int_m^{E_0} dE\sqrt{E^2-m^2}E(E_0-E)^2 \cdot K}{\int_m^{E_0} dE\sqrt{E^2-m^2}E(E_0-E)^2}, \tag{86}$$

where $d\lambda_0/dE$ is the differential transition rate in the absence of external fields. In the presence of a potential $V = -|V|$ (chosen negative for definiteness), the actual measured power would be given by

$$P = N \cdot \left[\int_m^{E_0} dE \frac{d\lambda_0}{dE} \cdot K + \int_m^{E_0+|V|} dE\delta\left(\frac{d\lambda}{dE}\right) \cdot K\right] \tag{87}$$

$$= N \cdot \lambda_0 \cdot \left[\overline{K}_0 + \frac{1}{\lambda_0}\int_m^{E_0+|V|} dE\delta\left(\frac{d\lambda}{dE}\right) \cdot K\right]. \tag{88}$$

Note that (86) was used in obtaining (88) from (87). Using $\overline{K} = \overline{K}_0$ in (84), combining it with (85) and (88), and then expanding to first order in $(\lambda_{\rm count} - \lambda_0)/\lambda_0$, we find that

$$\frac{\lambda_{\rm cal}}{\lambda_{\rm count}} = 1 + \frac{1}{\overline{K}_0\lambda_0}\int_m^{E_0+|V|} dE\delta\left(\frac{d\lambda}{dE}\right) \cdot (K - \overline{K}_0). \tag{89}$$

A similar result holds for a positive potential $V = +|V|$. We see that the calorimetric method yields a decay parameter which could differ from the true value $\lambda = \lambda_{\rm count}$. This discrepancy is solely due to the use of $\overline{K}_0$ in (85), which is no longer valid if the decay parameter is modified by an external field. While fractional count-rate modifications significantly larger than those indicated in Sects. 2 and 3 would be required to explain the $\sim 5\%$ discrepancies present in the ^{14}C literature, these considerations nonetheless underscore the point made earlier in Sect. 4: it is necessary to exercise care when comparing half-life measurements using different techniques, when the decay parameter λ is influenced by an external source.

^{14}C decays are particularly interesting from the present point of view because of the extensive literature comparing ^{14}C dates and tree-ring dates. Here we note that the tree-ring record presents a cumulative memory of not only the time-dependent production rate of ^{14}C, but also of its possible time-dependent decay if $\lambda(t)$ is not a constant. Specifically, an event such as the 1859 solar storm (Odenwald and Green 2008) could in principle influence the decay rate of the ^{14}C atoms already embedded in a tree ring sample, but not more recent atoms. Given improving ^{14}C dating techniques it may be of interest to search for evidence of major storms by looking for possible shifts in ^{14}C trend lines, as discussed in Sect. 4.

9 Ongoing and Future Experiments

We present in this Section a brief discussion of several experiments, both ongoing and future, with which our group is presently involved. We will defer for the present a discussion of experiments by other groups which are in progress or being planned. The experiments we discuss include generic searches for a time-dependence of the decay parameter $\lambda(t)$, as well as experiments which depend specifically on the suggestion that solar neutrinos may be the source of time-variation in the count-rates seen in the BNL/PTB data.

1. A long-term study of the decay of ^{54}Mn is underway at Purdue. The results of Sect. 3 suggest that ^{54}Mn decay may be sensitive to perturbations originating from the Sun, and this suggestion is qualitatively supported by the data we have acquired since December 2006. In contrast to Dec. 2006, which was a period of considerable solar activity, the period since then has been unusually quiet (Phillips 2009). No solar flares of equal or greater magnitude have been detected since then. Interestingly, our ^{54}Mn data have largely tracked solar behavior: although we recorded a number of dips in the December 2006 ^{54}Mn data (see Fig. 8), the recent count-rate in this experiment has been devoid of any significant fluctuations. At present a second experiment studying ^{54}Mn is running at a different location at Purdue with the aim of studying possible correlations between the two detectors.
2. As we have discussed above, one possible explanation of the dip in our ^{54}Mn count-rate during the solar flare of 2006 December 13 is that it arose from a fluctuation in the flux of solar neutrinos during the flare. In January 2007 we attempted to test this hypothesis by carrying out an experiment at the Brezeale Triga Reactor located at Pennsylvania State University. Although it is natural to suppose that exposing a radioactive sample to the flux of $\bar{\nu}_e$ from a reactor would be a straightforward test of the proposed neutrino mechanism, the practicalities of carrying out such an experiment proved to be more complex. In order to achieve a sufficiently high neutrino flux to provide a meaningful test, the radioactive samples had to be positioned as close to the core as possible. This produced a larger-than-expected γ-background, so the results of this run were inconclusive. We plan to repeat this experiment with a substantial increase in shielding in the near future.

   Another way to circumvent this problem is to have the sample of ^{54}Mn directly adjacent to the core, but without the associated electronics. The idea here is to irradiate the ^{54}Mn sample long enough to produce a sufficient suppression of the decay rate that the shift in decay curves shown in Fig. 9 becomes detectable when the sample is removed and counted. We are in the process of estimating how long an exposure would be required to produce a detectable effect. As noted above, the data collected during the flare of 2006 December 13 indicated that the fractional change in counting rate expected would have been only $\sim 10^{-5}$, which is below our detection sensitivity. To suppress the effects of neutrons transmuting the ^{54}Mn sample in such an experiment, the sample could be contained in borated polyethylene (HDPE) surrounded by cadmium to absorb neutrons. Since transmutation would in any case decrease the ^{54}Mn population and hence the count-rate, whereas the neutrino flux might work in the opposite direction, these two effects could presumably be disentangled. We are helped by the fact that the sequence $n + {}^{54}\mathrm{Mn} \rightarrow {}^{55}\mathrm{Mn}$ followed by $n + {}^{55}\mathrm{Mn} \rightarrow {}^{56}\mathrm{Mn}$ produces ^{56}Mn with $T_{1/2} = 2.58$ h. The decay of ^{56}Mn produces photons at 846.8 keV and 1810.8 keV and these can be used to estimate the neutron flux into the sample. The neutron flux can also be determined by placing gold foils near the sample and then measuring their neutron-induced activity. Photonuclear reactions involving the ^{54}Mn sample will also be present but with a low cross-section.

To summarize, the search for displaced decay curves is an attractive experiment because if an effect were seen this could in principle provide a quantitative estimate of the contribution of changing neutrino flux on decay rates.

3. We are in the process of carrying out a potentially cleaner test of the neutrino hypothesis in which the source of neutrinos is the decaying sample itself (Lindstrom et al. 2009; Fischbach et al. 2009). In this experiment the decay rates of two samples of ^{198}Au($T_{1/2} = 2.7$ d) are compared, where one sample is a thin foil and the other is a sphere of the same mass and approximate activity. It can be shown that the ratio of the sphere and foil decay rates from this "Self-Induced Decay" (SID) effect is given by ($x = t \ln 2/T_{1/2}$)

$$f(x,\alpha) = \frac{(dN/dt)_{\text{sphere}}}{(dN/dt)_{\text{foil}}} = \frac{1+\alpha}{[1+\alpha(1-\mathrm{e}^{-x})]^2}\frac{N_s}{N_f}. \tag{90}$$

Here N_s and N_f are the numbers of ^{198}Au atoms initially present in the sphere and foil respectively, and $\alpha = \delta\Gamma/\Gamma|_{t=0}$. As noted in Fischbach et al. (2009), the functional form of (90) can be understood as follows: initially the decay rate in the sphere exceeds that in the foil. However, by $t \approx T_{1/2}$ the resulting increase in the depletion of the population of decaying atoms in the sphere leads to an overall suppression of the decay rate in the sphere compared to that in the foil. An experiment to search for a nonzero contribution proportional to α in (90) is presently underway at the National Institute of Standards and Technology (Lindstrom et al. 2009), and this will eventually set a limit on α for incident $\bar{\nu}_e$.

4. Since the SID effect described above, and the reactor experiment described previously, set limits on the couplings on $\bar{\nu}_e$ but not on other neutrino species, it is of interest to consider experiments which might provide information on the contributions from ν_μ and ν_τ and/or their antiparticles. One possibility is to search for a day/night variation in count-rates which could arise from flavor oscillations as neutrinos pass through the Earth. To date there is no evidence for a day/night effect in our data. Another possibility is to look for a fluctuation in count-rates during a solar eclipse. Interestingly data on ^{137}Cs decay that we obtained during the solar eclipse of 2005 April 08 hinted at an effect, and this served as part of the motivation for a series of experiments we carried out at the Thule Air Base in Greenland during the eclipse of 2008 August 01. The Solar Eclipse at Thule (SEAT) collaboration was a joint effort of the U.S. Air Force Academy, Purdue Air Force ROTC, and the Purdue Physics Department, and collected an extensive set of data on a number of nuclides, which are presently being analyzed.
5. From the discussion in Sect. 4, the presence of extended "flat regions" is evidence for a time-varying decay parameter. Although there is nothing inherently more important about a "flat region" compared to any other "anomalous slope region", flat regions represent a potentially interesting confluence between an effect which is easy to spot, and a theoretical formalism for describing the data. From our ^{54}Mn data, flat regions may appear more frequently than solar flares. We propose to have several identical experiments running at different locations, and if flat regions were observed over the same time interval in two or more widely separated experiments this could be strong evidence for the presence of a time-dependence of $\lambda(t)$.

10 Implications for Detecting the Relic Neutrino Background

If the BNL/PTB data discussed in Sect. 2, and the solar flare data presented in Sect. 3, are in fact due to variations in the flux of solar neutrinos, then one implication of the present work

is that radioactive nuclides could serve as real-time neutrino detectors for some purposes. In principle, such "radionuclide neutrino detectors" (RNDs) could be combined with existing detectors, such as Super Kamiokande, to significantly expand our understanding of both neutrino physics and solar dynamics.

One potentially interesting application of such an RND would be to the detection of the predicted 1.95 K background of relic neutrinos which decoupled around 1 second after the Big Bang. This would be exciting, given that all previous proposals to detect the relic neutrino sea seem to be impractical at present (Duda et al. 2001). It is promising that the density of relic neutrinos is expected to be roughly 56 cm^{-3} per species for a total of 330 cm^{-3}, which is larger than the solar neutrino density at Earth. If we assume that the average speed of the Earth relative to the relic neutrino sea (or equivalently the cosmic microwave background) is $\sim$370 $km{\cdot}s^{-1}$, then the resulting flux of neutrinos incident on an RND would be $\sim 1 \times 10^{10}$ $cm^{-2}\,s^{-1}$. This is comparable to the estimated solar flux, $\sim 6 \times 10^{10}$ $cm^{-2}\,s^{-1}$, and potentially comparable to the fluctuation in the neutrino flux detected during the solar flare period discussed in Sect. 3.

The Earth's motion around the Sun results in the sinusoidal variation of its speed through the cosmic microwave background. Using the results of Kogut et al. (1993) and Gelmini and Gondolo (2001), one can show that the amplitude of this variation is $\sim$ 29 km/s, and that the Earth's peak speed occurs at around December 10. It is possible that this modulation could be detected in the signal of a decaying nuclear sample.

There are, however, important differences between the Earth's motion through the solar neutrinos compared to the relic neutrinos. Even if the relic neutrinos are galactically clustered, their density across the solar system should be almost completely uniform. Thus, unlike the case of our annual motion through the solar neutrinos, there would be no annual modulation in the density or flux of relic neutrinos. (The difference in number density due to differential Lorentz contraction throughout the year is completely negligible.) It follows that unless the interaction in question depends on the Earth's velocity through the sea of relic neutrinos, perhaps in a manner similar to the Stodolsky effect (Stodolsky 1975), there may be no annual modulation in decay rates due to such neutrinos. If the interaction in question is significantly energy-dependent, then the slight annual variation in relic neutrino energy seen by a nuclear sample could potentially affect the decay rate. However, the expected mean relic neutrino momentum is approximately 10^{-4} eV, compared to roughly 1 MeV for solar neutrinos. Thus, the relic-neutrino signal may be unobservably small in such a case.

Another difference is that solar neutrinos all have the same spin-orientation as detected on the Earth, whereas the relic neutrino background is unpolarized in the rest frame of the cosmic microwave background, and only very slightly polarized in the frame of the Earth. While this should make little difference for a short-ranged interaction, if the interaction in question is spin-dependent and sufficiently long-ranged, the nucleus (or any of its decay products) may experience a large number of simultaneous interactions which largely cancel. Furthermore, the relic neutrino background is expected to have roughly equal numbers of particles and antiparticles, and if these give potentials of opposite sign, a long-ranged interaction may result in an effect which largely cancels.

Nonetheless, in view of the current state of ignorance regarding the nature of the ν-nucleon interaction in question, it is perhaps not unreasonable to consider performing an experiment. Given that a signal due to relic neutrinos is likely to be quite small, one might need a very well controlled experiment with extremely high statistics. A modulation in count-rate data in phase with $\sim$ December 10/June 10 might indeed be a signature of the relic neutrino background. However, we note that our maximum speed through the relic neutrino background is coincident with our minimum speed through the galactic rest frame to within

$\sim$1 week. Thus, unless the experimental data allow for a phase resolution on the order of several days or less, it may be difficult to uniquely ascribe an observed signal to the relic neutrino background, as opposed to some other galactic effect, such as the WIMP interaction sought in the DAMA experiment (Bernabei et al. 2008). That said, a detection of any signal in this manner, whether due to neutrinos or WIMPs, would represent an exciting experimental result.

11 Summary and Conclusions

Our objective in this paper has been to present as complete a picture as possible of previous and current research dealing with the question of whether nuclear decay rates are being perturbed by some as yet unknown mechanism or new force. By "unknown" we mean to exclude phenomena associated with the more-or-less well-understood response of electron-capture processes to changes in the external environment, as discussed in Sect. 1. The motivation for embarking on this investigation comes from the following observations:

1. Evidence for a correlation between nuclear decay rates and Earth–Sun distance, as reported by the BNL and PTB groups (Sect. 2).
2. Detection of dips in the ^{54}Mn count-rate coincident in time with the solar flare of 2006 December 13 (Sect. 3).
3. Observation of "anomalous slope regions", particularly "flat regions" in the ^{54}Mn data taken at Purdue, and perhaps in the PTB data as well.
4. A history of reports of periodic effects in nuclear decays as reported by other groups (Table 1).
5. The existence of a significant number of discrepancies in half-life determinations by different groups, using either the same or different techniques (Sects. 2 and 4).
6. The possibility that the same mechanism which could account for the BNL/PTB data and the 2006 December 13 flare data, could also account for the apparently negative value of m_ν^2 inferred from ^{3}H decay (39)–(41).

Although it may eventuate that some or all of these effects arise from conventional (but presumably not-understood) systematic effects, the fact that so many effects have been reported in the literature by well-known and respected groups, suggests that we treat this problem seriously at present.

Even if we assume that most or all of the reported data are correct, it does not necessarily follow that nuclear decay rates themselves are being affected, as distinguished from the observed count-rates. Stated otherwise, it is possible (for example) that solar activity is affecting our instrumentation so as to simulate a time-varying decay-rate. Even if this were the case, for some purposes this could be quite interesting and useful: as we note in Sect. 3, there was a precursor signal in the ^{54}Mn count-rate that preceded the actual flare of 2006 December 13. From a practical point of view the possibility of using such a signal to warn of an impending flare is interesting irrespective of what the underlying mechanism might be.

Much of the present paper has been devoted to understanding how solar activity could in fact provide a non-trivial mechanism to account for the data, as we discuss in detail in Sects. 5 and 6. The conceptually simpler of the two mechanisms, which we discuss in Sect. 6, is one based on a variation of fundamental dimensionless constants such as $\alpha_{\rm EM}$ and m_e/m_p arising from some new field emanating from the Sun. Although we do not have a specific version of such a model at present which would be compatible with existing data, there is also no compelling argument precluding such a model.

The mechanism to which we have devoted most of our attention is a fluctuation in the flux of solar neutrinos, as discussed in Sect. 5. Perhaps the most compelling argument for such a mechanism are the data in Sect. 3 indicating dips in the ^{54}Mn count-rate coincident in time with a solar flare. In particular, the flare of 2006 December 13, which occurred at 21:37 EST where the data were taken, appear to require a mechanism in which a signal from the Sun travels through the Earth at approximately the speed of light in order to reach our detectors coincident in time with the flare. Since this would be compatible with a change in the solar neutrino flux, but not with some other mechanisms, this observation has served as part of the motivation for our proposed mechanism. Regrettably, in the event of a short-range neutrino interaction, the technical problems we have encountered in trying to implement this model have not yet been solved, and so in this case we do not have a completely formulated mechanism at present. However, for a sufficiently long-ranged solar-neutrino interaction, a potentially viable mechanism to explain the experimental data is presented in Sect. 5.3.

Even in the absence of a theoretical mechanism, there is nothing precluding us from studying time-varying nuclear decay parameters phenomenologically, along the lines described in Sects. 4 and 9, and we are in the process of doing this through a variety of experiments. In designing new experiments, and/or analyzing earlier experiments, it is important to bear in mind one of the important lessons from Sect. 4: in the presence of a time-varying decay parameter $\lambda(t)$ different experiments which have been carried out correctly can nonetheless legitimately infer different values for $T_{1/2}$ depending on the experimental technique and on the time interval over which the data were acquired. This observation could conceivably explain some of the discrepancies noted in point 5 above. Some of the experiments that are in progress are variants of existing experiments measuring half-lives of different nuclides, while others such as the SID effect and the SEAT experiment are conceptually new. Given the likelihood of increased solar activity in the next few years, the possibility of detecting solar flares via the effects they produce in decay rates of nuclei is quite exciting, and would be all the more exciting if several experiments around the world were running at the same time.

Acknowledgements The authors are deeply indebted to D. Alburger and G. Harbottle for supplying us with the raw data from the BNL experiment, to H. Schrader for providing to us the raw PTB data, and to A. Hall and M. Fischbach for their many contributions during the early stages of this collaboration. We also express our appreciation to D. Anderson, V. Barnes, P. Belli, R. Bernabei, B. Budick, R. Chrien, B. Craig, T. Downar, D. Elmore, A. Fentiman, V. Flambaum, Y. Fujii, G. Greene, J. Heim, M. Jones, A. Karam, A. Lasenby, R. Lindstrom, L. Lobashev, A. Longman, E. Merritt, T. Mohsinally, D. Mundy, P. Muzikar, A. Overhauser, L. Polsky, R. Reifenberger, S. Revankar, B. Revis, J. Schweitzer, M. Sloothaak, S. Soloway, P. Sturrock, R. Sutter, N. Titov, A. Treacher and J. Uzan, for their assistance and for many helpful conversations. The work of E.F. was supported in part by the U.S. Department of Energy under Contract No.DE-AC02-76ER071428.

References

E.G. Adelberger, E. Fischbach, D.E. Krause, R.D. Newman, Constraining the couplings of massive pseudoscalars using gravity and optical experiments. Phys. Rev. D **68**(6), 062002 (2003). doi:10.1103/PhysRevD.68.062002

D.E. Alburger, G. Harbottle, E.F. Norton, Half-life of ^{32}Si. Earth Planet. Sci. Lett. **78**, 168–176 (1986)

C. Amsler et al., Particle data group. Phys. Lett. B **667**(1) (2008)

J. Anderson, G. Spangler, Serial statistics: is radioactive decay random? J. Phys. Chem. **77**(26) (1973)

J.D. Barrow, D.J. Shaw, Varying alpha: New constraints from seasonal variations. Phys. Rev. D **78**(6), 067304 (2008). arXiv:0806.4317v1 [hep-ph]

Y.A. Baurov et al., Experimental investigation of changes in β-decay rate of ^{60}Co and ^{137}Cs. Mod. Phys. Lett. A **16**, 2089–2101 (2001)

Y.A. Baurov et al., Experimental investigation of changes in beta-decay count rate of radioactive elements. Phys. At. Nucl. **70**(11), 1825–1835 (2007)
H. Becquerel, On the invisible rays emitted by phosphorescent bodies. Comptes Rendus **122**, 501–503 (1896)
F. Begemann, K. Ludwig, G. Lugmair, K. Min, L. Nyquist, P. Patchett, P. Renne, C.Y. Shih, I. Villa, R. Walker, Call for an improved set of decay constants for geochronological use. Geochim. Cosmochim. Acta **65**(1), 111–121 (2001)
V. Berestetskii, E. Lifshitz, L. Pitaevskii, *Relativistic Quantum Theory, Part 2* (Pergamon, Oxford, 1979), pp. 402–408
R. Bernabei et al., First results from DAMA/LIBRA and the combined results with DAMA/NaI. Eur. Phys. J. C **56**, 333–355 (2008)
H. Bethe, Possible explanation of the solar neutrino puzzle. Phys. Rev. Lett. **56**(12), 1305–1308 (1986)
N. Bogoliubov, D. Shirkov, *Introduction To The Theory of Quantized Fields* (Wiley, New York, 1959), pp. 260–262
G.W. Bruhn, Does radioactivity correlate with the annual orbit of Earth around Sun? Aperion **9**(2), 28–40 (2002)
V. Chisté, M. Be, C. Dulieu, Evaluation of decay data of radium-226 and its daughters, in *Proceedings of the International Conference on Nuclear Data for Science and Technology, April 22–27, 2007, Nice, France*, ed. by O. Bersillon, F. Gunsing, E. Bauge, R. Jacqmin, S. Leray. (EDP Sciences, France, 2008). doi:10.1051/ndata:07122. http://nd2007.edpsciences.org/
T.C. Chiu, R. Fairbanks, L. Cao, R. Mortlock, Analysis of the atmospheric ^{14}C record spanning the past 50,000 years derived from high-precision ^{230}Th/^{234}U/^{238}U, ^{231}Pa/^{235}U and ^{14}C dates on fossil corals. Quart. Sci. Rev. **26**, 18–36 (2007)
P. Christmas, R.A. Mercer, M.J. Woods, S.M. Judge, ^{210}Bi and the apparent half-life of a sealed ^{226}Ra source. Int. J. Appl. Radiat. Isot. **34**(11), 1555 (1983)
P.S. Cooper, Searching for modifications to the exponential radioactive decay law with the Cassini spacecraft. Astropart. Phys. **31**(4), 267–269 (2009). arXiv:0809.4248v1 [astro-ph]
A. Derbin et al., Comment on the paper "realization of discrete states during fluctuations in macroscopic processes". Phys. Usp. **43**(2), 199–202 (2000)
G. Duda, G. Gelmini, S. Nussinov, Expected signals in relic neutrino detectors. Phys. Rev. D **64**, 122001 (2001)
K.J. Ellis, The effective half-life of a broad beam ^{238}PuBe total body neutron irradiator. Phys. Med. Biol. **35**(8), 1079–1088 (1990)
G.T. Emery, Perturbation of nuclear decay rates. Ann. Rev. Nucl. Phys. **22**, 165–202 (1972)
E.D. Falkenberg, Radioactive decay caused by neutrinos? Aperion **8**(2), 32–45 (2001)
E.D. Falkenberg, Reply to "Does radioactivity correlate with the annual orbit of Earth around Sun?" by G.W. Bruhn. Aperion **9**(2), 41–43 (2002)
L. Fassio-Canuto, Neutron beta decay in a strong magnetic field. Phys. Rev. **187**(5), 2141 (1969)
E. Fischbach, C. Talmadge, *The Search for Non-Newtonian Gravity* (Springer, New York, 1999)
E. Fischbach, D.E. Krause, New limits on the couplings of light pseudoscalars from equivalence principle experiments. Phys. Rev. Lett. **82**(24), 4753–4756 (1999a). doi:10.1103/PhysRevLett.82.4753
E. Fischbach, D.E. Krause, Constraints on light pseudoscalars implied by tests of the gravitational inverse-square law. Phys. Rev. Lett. **83**(18), 3593–3596 (1999b). doi:10.1103/PhysRevLett.83.3593
E. Fischbach et al., *Possibility of a Self-induced Contribution to Nuclear Decays*, 2009 ANS Proceedings (2009, in preparation)
V.V. Flambaum, E.V. Shuryak, How changing physical constants and violation of local position invariance may occur? in *AIP Conf. Proc.*, vol. 995, 2008, pp. 1–11
H. Frauenfelder, E.M. Henley, *Subatomic Physics*, 1st edn. (Prentice-Hall, New Jersey, 1974)
M. Fukugita, T. Yanagida, *Physics of Neutrinos and Applications to Astrophysics* (Springer, Berlin, 2003), p. 181
W. Furry, On bound states and scattering in positron theory. Phys. Rev. **81**(1), 115–124 (1951)
G. Gelmini, P. Gondolo, Weakly interacting massive particle annual modulation with opposite phase in late-infall halo models. Phys. Rev. D **64**, 023504 (2001)
D. Griffiths, *Introduction to Elementary Particles* (Wiley, New York, 1987)
H.P. Hahn, H.J. Born, J. Kim, Survey on the rate of perturbation of nuclear decay. Radiochim. Acta **23**, 23–37 (1976)
G. Harbottle, C. Koehler, R. Withnell, A differential counter for the determination of small differences in decay rates. Rev. Sci. Inst. **44**(1), 55–59 (1973)
P.E. Hodgson, E. Gadioli, E.G. Erba, *Introductory Nuclear Physics* (Clarendon, Oxford, 1997), p. 375
R. Horvat, Recent results of the neutrino mass squared measurements and the coherent neutrino–cold-dark-matter interaction. Phys. Rev. D **57**(8), 5236 (1998)

J. Jenkins, E. Fischbach, Perturbation of nuclear decay rates during the solar flare of 13 December 2006. arXiv:0808.3156v1 [astro-ph] (2008)
J. Jenkins et al., Evidence for correlations between nuclear decay rates and Earth–Sun distance. arXiv:0808.3283v1 [astro-ph] (2008)
V.R. Khalilov, Electroweak nucleon decays in a superstrong magnetic field. Theor. Math. Phys. **145**(1), 1462 (2005)
A. Kogut et al., Dipole anisotropy in the COBE differential microwave radiometers first-year sky maps. Apstrophys. J. **419**, 1–6 (1993)
B.F. Kostenko, M.Z. Yuriev, Possibility of a modification of life time of radioactive elements by magnetic monopoles. Ann. Found. L. de Broglie **33**(1–2), 93–106 (2008). arXiv:0709.1052v1 hep-ph
E.A. Kushnirenko, I.B. Pogozhev, Comment on the paper by S.E. Shnoll et al. Phys. Usp. **43**(2), 203–204 (2000)
R. Lindstrom et al., *Does the Half-Life of a Radioactive Sample Depend on Its Shape*? 2009 ANS Proceedings (2009, in preparation)
V. Lobashev et al., Direct search for mass of neutrino and anomaly in the tritium beta-spectrum. Phys. Lett. B **460**, 227–235 (1999)
V. Lyul'ka, Elementary particle decays in the field of an intense electromagnetic wave. Sov. Phys.-JETP **42**(3), 408–412 (1975)
F. Mandl, G. Shaw, *Quantum Field Theory–Revised Edition* (Wiley, New York, 1993), pp. 159–165
J.J. Matese, R.F. O'Connell, Neutron beta decay in a uniform constant magnetic field. Phys. Rev. **180**(5), 1289 (1969)
J. Nieves, Neutrinos in a medium. Phys. Rev. D. **40**(3), 866–872 (1989)
A. Nikishov, V. Ritus, Quantum processes in the field of a plane electromagnetic wave and in a constant field. Sov. Phys.-JETP **19**(5), 1191–1199 (1964)
NNDC, 2008. http://www.nndc.bnl.gov/qcalc
NOAA, 2005. http://www.swpc.noaa.gov/NOAAscales/index.html
NOAA, NOAA Space Environment Center, SEC PRF 1634, 2006
NOAA, 2009. http://www.ngdc.noaa.gov/stp/
E. Norman et al., Influence of physical and chemical environments on the decay rates of ^{7}Be and ^{40}K. Phys. Lett. B **519**, 15–22 (2001)
E.B. Norman et al., Evidence against correlations between nuclear decay rates and Earth–Sun distance. Astropart. Phys. **31**, 135–137 (2009)
S.F. Odenwald, J.L. Green, Bracing for a solar superstorm. Sci. Am. **299**(2) (2008)
B. Odom, D. Hanneke, B. D'Urso, G. Gabrielse, New measurement of the electron magnetic moment using a one-electron quantum cyclotron. Phys. Rev. Lett. **97**, 030801 (2006)
T. Ohtsuki, H. Yuki, M. Muto, J. Kasagi, K. Ohno, Enhanced electron-capture decay rate of ^{7}Be encapsulated in C_{60} cages. Phys. Rev. Lett. **93**, 112501 (2004)
A.G. Parkhomov, Bursts of count rate of beta radioactive sources during long-term measurements. Int. J. Pure Appl. Phys. **1**, 119–128 (2005)
T. Phillips, 2009. http://science.nasa.gov/headlines/y2009/01apr~deepsolarminimum.htm
S. Pommé, Problems with the uncertainty budget of half-life measurements. Am. Chem. Soc. Symp. Ser. **945**, 282–292 (2007)
S. Pommé, J. Camps, R. Van Ammel, J. Paepen, Protocol for uncertainty assessment of half-lives. J. Rad. Nucl. Chem. **276**(2), 335–339 (2008)
H.R. Reiss, Nuclear beta decay induced by intense electromagnetic fields: Basic theory. Phys. Rev. C **27**(3), 1199 (1983)
V. Ritus, Effect of an electromagnetic field on decays of elementary particles. Sov. Phys.-JETP **29**(3), 532–541 (1969)
T. Rosenband et al., Frequency ratio of Al^{+} and Hg^{+} single-ion optical clocks; metrology at the 17th decimal place. Science **319**, 1808 (2008)
E. Rutherford, *Radioactive Substances and Their Radiations* (Cambridge University Press, New York, 1913)
E. Rutherford, J. Chadwick, C. Ellis, *Radiations from Radioactive Substances* (Cambridge University Press, Cambridge, 1930), p. 167
A.J. Sanders, Implications for C-14 dating of the Jenkins-Fischbach effect and possible fluctuation of the solar fusion rate (2008). arXiv:0808.3986v2 [astro-ph]
H. Schrader, Private communication, 2008
D.J. Shaw, Detecting seasonal changes in the fundamental constants (2007). arXiv:gr-qc/0702090v1
S.E. Shnoll et al., Realization of discrete states during fluctuations in macroscopic processes. Phys. Usp. **41**, 1025–1035 (1998)
S.E. Shnoll et al., Regular variation of the fine structure of statistical distributions as a consequence of cosmophysical agents. Phys. Usp. **43**(2), 205–209 (2000)

H. Siegert, H. Schrader, U. Schötzig, Half-life measurements of europium radionuclides and the long-term stability of detectors. Appl. Radiat. Isot. **49**(9–11), 1397 (1998)
M. Silverman, W. Strange, C. Silverman, T. Lipscombe, On the run: Unexpected outcomes of random events. Phys. Teach. **37**, 218–225 (1999)
M. Silverman, W. Strange, C. Silverman, T. Lipscombe, Tests for randomness of spontaneous quantum decay. Phys. Rev. A **61**(042106) (2000)
L. Stodolsky, Speculation on detection of the "neutrino sea". Phys. Rev. Lett. **34**(2), 110–112 (1975)
W. Stoeffl, D.J. Decman, Anomalous structure in the beta decay of gaseous molecular tritium. Phys. Rev. Lett. **75**(18), 3237 (1995)
P.A. Sturrock, Solar neutrino variability and its implications for solar physics and neutrino physics. Astrophys. J. **688**, 53 (2008)
J. Taylor, *An Introduction to Error Analysis* (University Science Books, Sausalito, 1997)
I.M. Ternov et al., β-decay polarization effects in an intense electromagnetic field. Sov. J. Nucl. Phys. **28**(6), 747 (1978)
I.M. Ternov et al., Polarization effects and electron spectrum in the nuclear β decay in the field of an intense electromagnetic wave. Sov. J. Nucl. Phys. **39**(5), 710 (1984)
S.J. Tu, E. Fischbach, Geometric random inner products: A family of tests for random number generators. Phys. Rev. E **67**, 016113 (2003)
S.J. Tu, E. Fischbach, A study on the randomness of the digits of π. Int. J. Mod. Phys. C **16**(2), 281–294 (2005)
J. Uzan, The fundamental constants and their variation: observational and theoretical status. Rev. Mod. Phys. **75**, 403–455 (2003)
F. Wissman, Variation observed in environmental radiation at ground level. Rad. Prot. Dos. **118**, 3–10 (2006)
C.S. Wu, S.A. Moszkowski, *Beta Decay* (Interscience, New York, 1966)